

Project acronym:	Geo-Drill		
Project title:	Development of novel and Cost-Effective drilling technology for geothermal Systems		
Activity:	LCE-07-17-Renewables		
Call:	H2020-LC-SC3-2018-RES-TwoStages		
Funding Scheme:	RIA	Grant Agreement No:	815319
WP 3	Material Testing and Characterization		

D3.7 – Report on materials testing and characterization

Due date:	30/06/2021 (M26)		
Actual Submission Date:	30/11/2021		
Lead Beneficiary:	TWI		
Main authors/contributors:	UoI, CSM-RINA, Gerosion EHF		
Dissemination Level¹:	PU		
Nature:	REPORT		
Status of this version:		Draft under Development	
		For Review by Coordinator	
	X	Submitted	
Version:	1.0		
Abstract	The deliverable provides an overview of the activities under WP3.		

REVISION HISTORY

Version	Date	Main Authors/Contributors	Description of changes
V1		TWI, UoI, CSM-RINA, Gerosion ENF	



This project has received funding from the *European Union's Horizon 2020 research and innovation programme* under grant agreement No 815319

¹ Dissemination level security:

PU – Public (e.g. on website, for publication etc.) / **PP** – Restricted to other programme participants (incl. Commission services) /

RE – Restricted to a group specified by the consortium (incl. Commission services) / **CO** – confidential, only for members of the consortium (incl. Commission services)



This project has received funding from the European Union's Horizon 2020 program Grant Agreement No 815319. This publication reflects the views only of the author(s), and the Commission cannot be held responsible for any use which may be made of the information contained therein.

Copyright © 2019-2023, Geo-Drill Consortium

This document and its contents remain the property of the beneficiaries of the Geo-Drill Consortium and may not be distributed or reproduced without the express written approval of the Geo-Drill Coordinator, TWI Ltd. (www.twi-global.com)

THIS DOCUMENT IS PROVIDED BY THE COPYRIGHT HOLDERS AND CONTRIBUTORS "AS IS" AND ANY EXPRESS OR IMPLIED WARRANTIES, INCLUDING, BUT NOT LIMITED TO, THE IMPLIED WARRANTIES OF MERCHANTABILITY AND FITNESS FOR A PARTICULAR PURPOSE ARE DISCLAIMED. IN NO EVENT SHALL THE COPYRIGHT OWNER OR CONTRIBUTORS BE LIABLE FOR ANY DIRECT, INDIRECT, INCIDENTAL, SPECIAL, EXEMPLARY, OR CONSEQUENTIAL DAMAGES (INCLUDING, BUT NOT LIMITED TO, PROCUREMENT OF SUBSTITUTE GOODS OR SERVICES; LOSS OF USE, DATA, OR PROFITS; OR BUSINESS INTERRUPTION) HOWEVER CAUSED AND ON ANY THEORY OF LIABILITY, WHETHER IN CONTRACT, STRICT LIABILITY, OR TORT (INCLUDING NEGLIGENCE OR OTHERWISE) ARISING IN ANY WAY OUT OF THE USE OF THIS DOCUMENT, EVEN IF ADVISED OF THE POSSIBILITY OF SUCH DAMAGE.

Summary

The following work was undertaken in this report:

- **T3.1 Mechanical testing and microstructural characterization of coupons**

Microstructural, mechanical, and dry PoD sliding test were carried out for T3.1. The 1-3 best performing coatings per coating group were selected for further testing at high temperatures and tribo-corrosion sliding tests. The Xylan+0.5wt% GO coating was chosen from the Xylan-GO coating group and the heat treated ENPs (at 300°C); HP-HP-PTFE 300 and HP-LP-PTFE 300. The HVOF coatings selected for further tests were the 233WC, 234Flux and 282WCr coatings. The main conclusions are the following:

- *The 80°C wet sliding test in water* showed a higher wear rate for the 0.5wt%GO compared to 0wt%GO but slightly lower CoF value was obtained for the 0.5wt%GO. The results for the ENPs from the 80°C wet sliding test correlated closely to the room temperature dry sliding test, i.e. the HP-LP-PTFE 300 has lower wear rate for both tests compared to HP-HP-PTFE 300.
- For the *tribo-corrosion test at RT in saline fluid* the results from the potentiodynamic polarization tests show a higher corrosion potential (E_{corr}) for the Xylan+0.5wt% GO compared to the neat Xylan (0wt% GO). The Xylan+0.5wt% GO also outperforms the neat Xylan (0wt% GO) after the combined corrosion and sliding test with lower wear volume measured and lower CoF. There is no significant difference in the obtained corrosion potential (E_{corr}) for both ENP coatings. However, neither coating showed passive behaviour, nevertheless the resulting corrosion current measured was very low (10^{-8} A/cm²). From the corrosion test, a similar trend was observed for the corrosion and sliding test for the ENPs. However, stability in the friction coefficient in both coatings was low. A slightly lower drop in potential was observed for the HP-LP-PTFE300°C.
- For the Xylan based compounds (0wt% and 0.5wt%), in the *tribo-corrosion test at 80°C in NS4 solution*, the effect of small polarization seems to have some influence with a modification of the material (more porosity) although the experiments have been conducted in a narrow potential interval close to E_{corr} generally considered safe. The modified Xylan (Xylan0.5wt%GO) looks worn out in the track area, while all analyzed coatings look detached from the substrate in the track area, where the material was stressed by the application of the load (10N). Far from the wear track zone the coating adhesion is good.
- The results from the *80°C wet sliding test in water* identified 282WCr as best performing coating with no measurable wear and outperformed the substrate. The results from the high temperature sliding wear tests of the 282WCr and 232WC at 340°C; and the BoR wear test at 650°C of 234Flux; showed that the coatings did not outperform the substrate (but 282Cr outperformed 232WC). For the *tribo-corrosion tests at RT in saline fluid* the 234Flux performed best out of the down-selected HVOF coatings with lowest OCP. In the *tribo-corrosion test at 80°C in NS4 solution* only the 282WCr and 232WC were tested where indications of corrosion reactions (oxides) during sliding were detected but the coatings outperformed the substrate material with less weight gain. Considering the HVOF coatings for components experiencing abrasive wear in drilling fluid the combined results from T3.1 indicate that the 282WCr and 234Flux showed best performance overall.

- **T3.2 Corrosion testing in simulated geothermal drilling environment**

Preliminary results from visual inspection and weight loss/gain analyse after corrosion testing show that:

- Samples with 0.5% GO Xylan-GO coated samples showed promising performance with least visible changes in coating appearance and weight change.

- The 282WCr; 233CrC and 283HEA samples were the best performing HVOF fabricated samples, with least visible changes in coating appearance compared to untested samples and for the 282WCr no crevice corrosion damages were visible.
- The ENP coatings had visible corrosion damages for all designed test conditions.
- The tested corrosion coupons were used for evaluating the corrosion resistance with microstructural and chemical compositional analysis performed in Task 3.5. The results were used for the ranking of the coatings to select the best coatings for the components of the prototypes of the novel DTH hammer developed and built in WP4.

- **T3.3 Erosion-corrosion testing in simulated geothermal drilling environment**

Erosion-corrosion testing of materials received from WP2 in simulated geothermal drilling environment is carried out, including:

- An erosion-corrosion testing facility using main elements of the slurry pot equipment (ASTM G119) was designed, with in-situ electrochemical measurement capabilities.
- Formulation of simulated geothermal drilling fluid was defined to carry out erosion-corrosion testing.
- Two rounds of erosion-corrosion testing was carried out at 24h and 7day duration in simulated drilling fluid. A total number of sixteen (16) samples were tested. From the results, samples 222Xylan/GO1 and 234Flux1 are proved to have good protection to Steel 1 in the selected testing condition. Steel 2 performs very well itself and is recommended not to have the need to be coated in similar drilling environment.

- **T3.4 HTHP testing and evaluation of sensor and cable material**

This task is dedicated for high temperature and high-pressure testing and evaluation of pre-selected materials for sensor and cable parts of the novel drilling technology.

- The selected materials performed well under standard drilling conditions based on failure analysis.
- When the conditions become more demanding, with temperature of 250°C and highly pressurised steam together with hot fluids, some materials start to underperform and result in material failure (degradation and breakage).
- Chemical resistance of the materials selected by PVI towards acids, base, and salts seems satisfactory from the testing and based on research/academic resources for standard drilling operations.
- Gerosion Ltd. recommends finding alternative materials for structural components for the accelerometer and pressure sensor devices if the sensor are desired to survive extremely demanding environments such as breach of geothermal fluids/accidents. Preselected failed material should be used as a last option and/or cooling should be implemented if operations are expected above “standard” drilling conditions. In case of using commercially available alternatives as the structural component the performance is expected to only improve in harsh conditions.

- **T3.5 Evaluation and ranking of developed materials and coatings**

Based on a) evaluation of the corrosion resistance of the coatings received from WP2 after corrosion testing in simulated geothermal drilling environment at elevated temperature and pressure in Task 3.2, and b) the ranking of the developed materials and coatings by best performance based on microstructural characterization, mechanical properties and corrosion and wear resistance measured in laboratory tests in Tasks 3.1, 3.3 and 3.4, ranking of developed materials and coatings in Geo-Drill is finalised below:

- The Xylan 0.5wt%GO is the most potential coating showing best performance among the Xylan based polymer coatings developed within Geo-Drill. Thus it should be tested further in-situ in DTH hammer prototype in WP4 where low friction is needed and erosion-corrosion can be encountered.
- The HVOF coating developed within the Geo-Drill recommended to be tested further in-situ for the first proto-type of the DTH hammer where high wear is encountered in water based drilling fluid for the protection of 34CrNiMo6 substrate is the 234Flux coating.
- The HP-LP-PTFE300 showed better performance than the HP-HP-PTFE300 coating with good corrosion and wear resistance at RT conditions but does poorly at higher temperatures and pressure which restrains the potential usage for geothermal drilling conditions.
- For the sensor material the selected materials performed well under standard drilling conditions based on failure analysis except the silicon material and the Kapton which showed decrease in ductility.

- **T3.6 Perform welding test on coupons**

Work in this task was carried out on welding processing including the following:

- Welding processes were reviewed in the context of the materials and geometry of the drill pipe components. Following the review, Rotary Friction welding was selected as the most suitable process.
- Parameters were selected to form a Design of Experiments (DoE) matrix for selected rotary friction welding process. All the welding parameters selected achieved a uniform, defect-free weld.
- Weld coupons were made using optimised parameters for testing of a WC-CoCr coating (36WC) and a self-fluxing coating (36Flux) coating. Results show that rotary friction welding process does not seem to have an impact on the coating integrity.
- This task has increased the consortium's understanding of the effect of welding on coating integrity.

Objectives Met

The work described contributes to the following WP3 objective:

- To perform microstructural characterization of the developed materials.
- To evaluate mechanical and tribological performances of the developed materials.
- To test the corrosion resistance of the developed materials in simulated geothermal drilling environment at elevated temperature and pressure.
- To evaluate different forms of corrosion (such as, general corrosion, pitting and erosion-corrosion) effect on the developed materials after the exposure of test coupons in simulated drilling environment.
- To test the sensor and 3D printed cable materials in high temperature and pressure.
- To evaluate the durability of the sensor and 3D printed cable material in simulated high temperature drilling environment.
- To rank the synthesized materials and coating after testing.

CONTENTS

SUMMARY.....	3
OBJECTIVES MET	5
1 INTRODUCTION	7
2 TASKS IN WP3.....	7
2.1 T3.1 MECHANICAL TESTING AND MICROSTRUCTURAL CHARACTERIZATION OF COUPONS	7
2.1.1 Microstructural analysis (Uol)	8
2.1.2 Mechanical Test	8
2.1.2.1 Hardness test (Uol).....	8
2.1.2.2 Adhesion Test (CSM/RINA).....	9
2.1.2.3 Scratch Test (CSM/RINA)	15
2.1.2.4 Slurry test (CSM/RINA)	19
2.1.3 Tribological test results	23
2.1.3.1 Pin-on-Disk dry rotating test at RT (Uol)	23
2.1.3.2 Pin-on-Disk wet rotating test at 80°C (Uol)	23
2.1.3.3 Reciprocated sliding test at RT and 340°C (CSM/RINA).....	24
2.1.3.4 Block-on-Ring test, RT & 650°C (CSM/RINA)	30
2.1.3.5 Trobi-corrosion test in saline fluid at RT (Uol)	34
2.1.3.6 Tribo-corrosion test in NS4 solution at 80°C (CSM/RINA)	34
2.2 T3.2 CORROSION TESTING IN SIMULATED GEOTHERMAL DRILLING ENVIRONMENT	59
2.3 T3.3 EROSION-CORROSION TESTING IN SIMULATED GEOTHERMAL DRILLING ENVIRONMENT	61
2.4 T3.4 HTHP TESTING AND EVALUATION OF SENSOR AND CABLE MATERIAL.....	61
2.5 T3.5 EVALUATION AND RANKING OF DEVELOPED MATERIALS AND COATINGS.....	63
2.6 T3.6 PERFORM WELDING TEST ON COUPONS	65
3 CONCLUSIONS	65
REFERENCES	66

1 INTRODUCTION

This report covers a range of activities for characterization and testing of developed materials and coatings in Geo-Drill. This include:

- Carrying out mechanical testing and microstructural characterization of test coupons
- Performing corrosion testing in simulated geothermal drilling environment
- Performing Erosion-corrosion testing in simulated geothermal drilling environment
- Carrying out high temperature and high pressure (HTHP) testing in simulated geothermal drilling environment
- Evaluating and ranking of developed materials and coatings
- Performing weld trials on test coupons

2 TASKS IN WP3

2.1 T3.1 Mechanical testing and microstructural characterization of coupons

The following objectives were performed within this task:

1. To perform microstructural characterization of the developed materials.
2. To evaluate mechanical and tribological performance of the developed materials from WP2.

The laboratory tests in Task 3.1 involved the following tests and analysis:

- Microstructural analysis of the as pre-prepared samples with X-ray diffraction analysis (XRD), Raman spectroscopy, optical and scanning electron microscopy (SEM) equipped with energy dispersive spectroscopy (EDS).
- Mechanical Test:
 - Hardness test on coatings and bulk materials from WP2
 - adhesion tests according to ASTM C633 standard and cross-cut test on selected coatings from WP2 and on the reference material
 - micro-hardness tests on coatings and bulk materials from WP2 and on the reference material
 - slurry test according to ASTM G75 standard on selected coatings from WP2 and on the reference material
- Tribological Tests:
 - Pin-on-disk (PoD) dry sliding at room temperature (RT) and PoD at 80°C in water
 - Reciprocated sliding test at RT & 340°C
 - Block-on-Ring test, at RT & 650°C
 - Tribo-corrosion tests were performed:
 - at RT in saline solution
 - at 80°C using selected mud

The microstructure and characterization of the samples after tribological/tribocorrosion tests were analysed by Profilometers/Optical Microscope/SEM/EDS/XRD equipment to evaluate the performance, e.g. to evaluate damage and calculate the wear rates.

The following results were obtained from the laboratory tests and analyses:

2.1.1 Microstructural analysis (Uoi)

From microstructural analyse:

- The Xylan-graphene oxide (GO) added coatings are based on the Xylan commercial coating consisting of a Polyphenylene sulfide (PPS) and Polytetrafluoroethylene (PTFE) and silica micro-particles. The graphene oxide particles are nano-platelets where their presence was identified and confirmed with Raman and XRD analysis. The results show that the GO added coating with more than 1wt% of GO have micro defects in the form of cracks and pores. The focus for further testing was then set on the 1wt% and lower graphene oxide (GO) coatings, particularly the 0.5wt% GO coatings.
- The Electroless Nickel Plating (ENP) coating with Polytetrafluoroethylene (PTFE) added particles have a bi-layer structure with a total thickness of 10-20 μm . The microstructural analysis with XRD and Raman showed that the two layered ENP coating with low phosphorus top coat and high phosphorus undercoat (LP-HP-PTFE) is crystalline, whereas that of the high phosphorus top coat and high phosphorus undercoat (HP-HP-PTFE) coating tends to a mixed crystalline-amorphous structure. But after heat treatment for 2 hours at 300 °C of the HP-HP-PTFE samples, additional Ni_3P phases were identified.
- All six coatings developed from the HVOF spraying technique have a dense microstructure, relatively smooth surface finish and a good mechanical bond between the coating and substrate except for the 235Amor coating where interfacial defects (cracks/pores) were detected in the cross-section at the interface. The HVOF technique produced coatings with thickness ranging between 200 – 400 μm . For the six coatings, 232WC had the highest thickness averaged as $395.8 \pm 17.8 \mu\text{m}$. No visible pores, cracks and delaminated areas were found across the thickness of the coatings except for the 235Amor.
- For the GO enhanced WC-Co sintered bulk samples the results from the microstructural analysis indicated that the sample with 9wt% GO addition to the WC-Co material is less dense and compact compared to the WC/5.6wt% reduced Graphene Oxide (rGO) added sample. The results identified a crystalline microstructure for the WC/5.6wt% rGO and the WC/9wt% GO with peaks identified as WC and Co. The results from Raman analysis of the WC-Co/9wt%GO, and WC-Co/5.6wt% rGO samples, confirmed the presence of the GO sheets. More interestingly, new peaks at around 700 cm^{-1} were detected which was attributed to the formation of an amorphous carbon -based cobalt phase.

2.1.2 Mechanical Test

2.1.2.1 Hardness test (Uoi)

From Hardness testing:

- The PTFE/PPS (Xylan)+GO added coatings are relatively thin and soft, thus the Knoop method was used with a low load. The hardness of the neat Xylan was comparable to the Xylan+GO coatings for the 0.5-2.5wt% but decrease in hardness was measured for the Xylan+5wt%GO coating, which is likely attributed to the existence of cracks and pores in the coating.
- The ENP coatings are also relatively thin and composed of two layers. The hardness of the coatings increased with the heat treatments. The HP-HP-PTFE coatings with and without heat treatments and the heat treated HP-LP-PTFE coating had higher hardness than the substrate material (34CrNiMo6). The HP-HP-PTFE coating heat treated at 300°C had the highest hardness ($474.12 \pm 87.77 \text{ HK0.05}$) among all the tested ENP coatings which was attributed to the formation of additional Ni_3P phases, identified in the microstructural analysis, and has been reported to improve the hardness of ENP coatings.

- All the HVOF coatings had higher hardness than the substrate material (34CrNiMo6) which was 292.6 ± 7.4 HV0.3 for comparison. The 232WC had the highest hardness, not surprisingly since the cermet composition is known for very high hardness, the 283HEA had the lowest hardness but still higher than substrate material.
- The hardness of the WC-Co with 9wt%GO bulk material could not be measured due to porous structure. Improvement in structural properties were achieved with the WC-Co-5.6wt% rGO samples, but the hardness value decreased approximately by a factor of 0.5 compared to the reference bulk sample prepared (WC-Co; 1028.87 ± 45.86 HV0.3). Despite this the lower coefficient of friction and wear rate was measured for the rGO enhanced WC-Co matrix, compared to the WC-Co.

2.1.2.2 Adhesion Test (CSM/RINA)

CSM/RINA performed adhesion test according to ASTM C633 to determinate the degree of adhesion to a substrate, or the cohesion strength of the coating after the application of a normal tension to the surface. The test consists of coating one face of a substrate fixture, adhesive bonding this coating to the face of a loading fixture, and subjecting this assembly to a tensile load normal to the plane of the coating using a tensile testing machine, Figure 2.1.1. Failure stress is calculated dividing the maximum load by the cross-sectional area of the specimen. Fractured surfaces are examined to determine the location of the failure in the specimen.

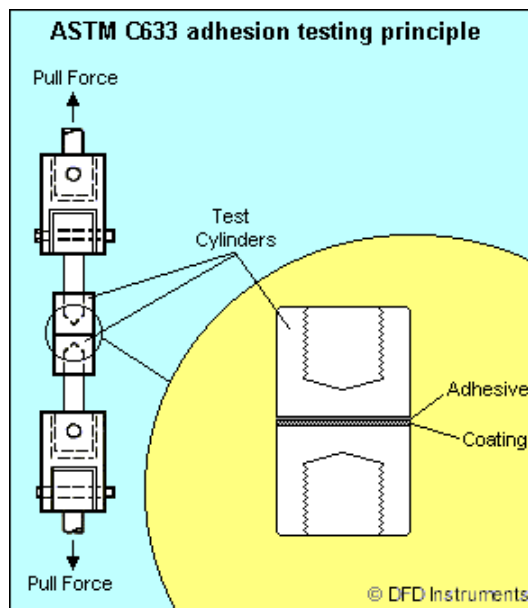


Figure 2.1.1 Standard ASTM C633 adhesion testing principle

RINA-CSM performed pull tests to ASTM C633 standards on the samples received from TWI listed in Table 2.1.1.

Table 2.1.1 - Summary of samples received to CSM from TWI for Adhesion tests

ID	Substrate	Geometry
232WC_A1	34CrNiMo6	
232WC_B1	X90CrMoV18	
233 CrC_A1	34CrNiMo6	
233 CrC_B1	X90CrMoV18	
234Flux_A1	34CrNiMo6	


234Flux_B1	X90CrMoV18	
235Amor_A1	34CrNiMo6	
235Amor_B1	X90CrMoV18	
282WCr_A1	34CrNiMo6	
282WCr_B1	X90CrMoV18	
283HEA_A1	34CrNiMo6	
283HEA_B1	X90CrMoV18	

Figure 2.1.2 shows some specimens after the gluing procedure.



Figure 2.1.2 - An example of samples after gluing

Following the gluing phase, the specimens were subjected to the pull test. The test was carried out in the RINA CSM laboratories following the scheme shown in Figure 2.1.1.

Due to the many variables that affect the adhesion test, the results of three repetitions were used for the calculation of the tensile strength [MPa]. Failure modes have been evaluated by visual inspection. A further test was also performed on uncoated specimens to determine the strength of the glue used, the results of this test are summarized in Table 2.1.2.

Table 2.1.2 - Glue Pull test results

Pull test - Glue	
Tensile Strength [MPa]	
Average	St. Dev.
70	3.8

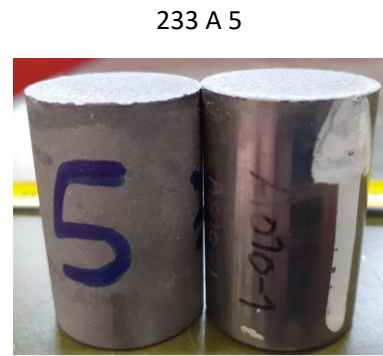
Figure 2.1.3 to Figure 2.1.14 show tested samples and comments about failure modes. The results of pull tests are summarized in Table 2.1.3.



Glue failure



Glue failure

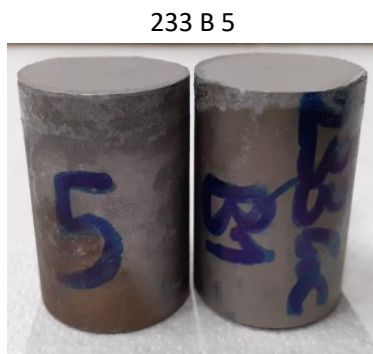


Glue failure

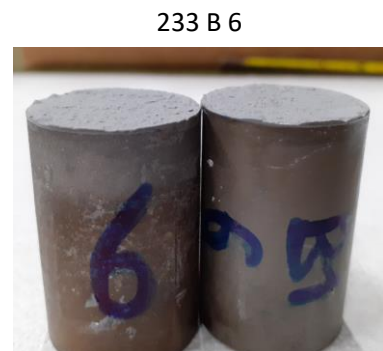
Figure 2.1.3 - 233 A Samples after pull test



Glue failure



Coating cohesion failure



Coating cohesion failure

Figure 2.1.4 - 233 B Samples after pull test



Glue failure



Coating cohesion failure



Coating cohesion failure

Figure 2.1.5 - 232 A Samples after pull test



Coating cohesion failure

232 B 3



Coating cohesion failure

232 B 5



Glue failure

Figure 2.1.6 - 232 B Samples after pull test

234 A 1



Dual failure mechanism due to both the adhesion of the coating and the failure of the glue

234 A 2



Dual failure mechanism due to both the adhesion of the coating and the failure of the glue

234 A 3



Dual failure mechanism due to both the adhesion of the coating and the failure of the glue

Figure 2.1.7 - 234 A Samples after pull test

234 B 2



Coating adhesion failure

234 B 5



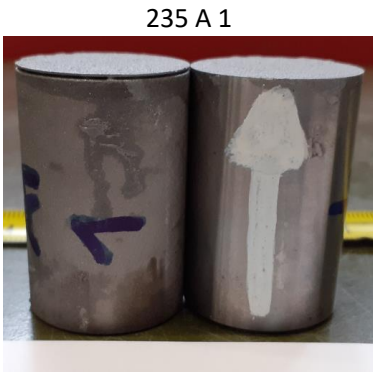
Coating adhesion failure

234 B 6

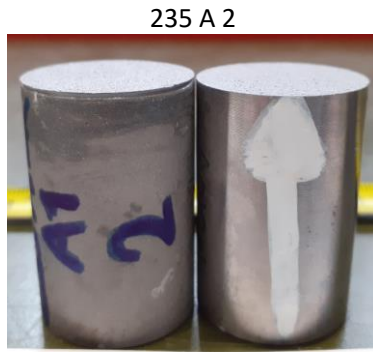


Coating adhesion failure

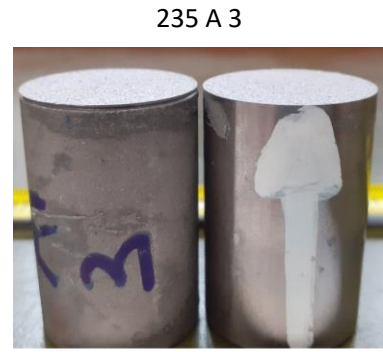
Figure 2.1.8 - 234 B Samples after pull test



Coating adhesion failure



Coating adhesion failure



Coating adhesion failure

Figure 2.1.9 - 235 A Samples after pull test



Coating adhesion failure

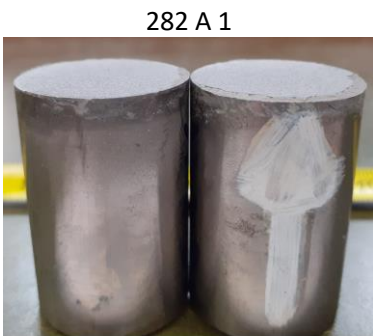


Coating adhesion failure

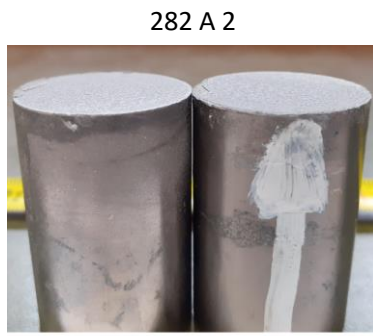


Coating adhesion failure

Figure 2.1.10 - 235 B Samples after pull test



Dual failure mechanism due to both the adhesion of the coating and the failure of the glue

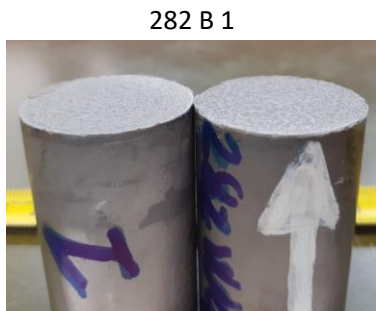


Dual failure mechanism due to both the adhesion of the coating and the failure of the glue

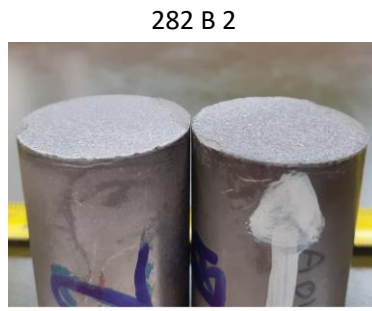


Dual failure mechanism due to both the adhesion of the coating and the failure of the glue

Figure 2.1.11 - 282 A Samples after pull test



Dual failure mechanism due to both the adhesion of the coating and the failure of the glue

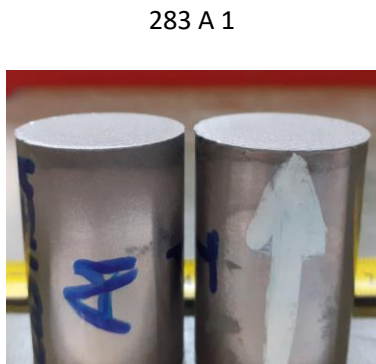


Dual failure mechanism due to both the adhesion of the coating and the failure of the glue

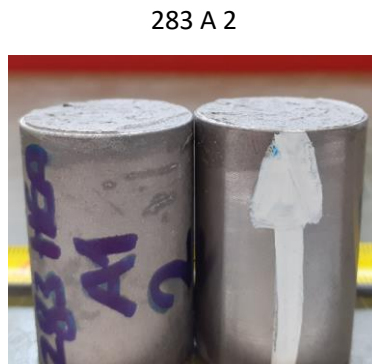


Dual failure mechanism due to both the adhesion of the coating and the failure of the glue

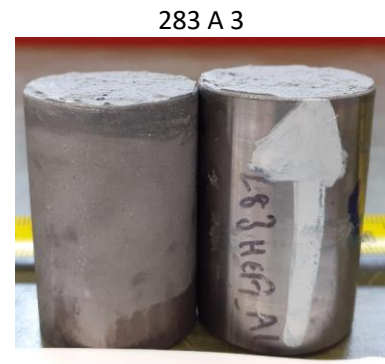
Figure 2.1.12 - 282 B Samples after pull test



Coating cohesion failure



Coating cohesion failure



Coating cohesion failure

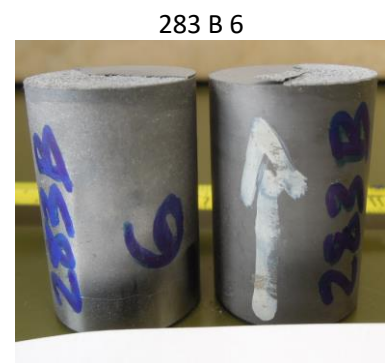
Figure 2.1.13 - 283 A Samples after pull test



Coating cohesion failure



Dual failure mechanism due to both the adhesion of the coating and the failure of the glue



Dual failure mechanism due to both the adhesion of the coating and the failure of the glue

Figure 2.1.14 - 283 B Samples after pull test

Table 2.1.3 – Pull tests results

	Pull test - A		Pull test - B	
	Tensile Strength (Mpa)		Tensile Strength (Mpa)	
	Ave.	St. Dev.	Ave.	St. Dev.
233 CrC	67.4	0.3	64.9	2.4
232Wc	64.2	4.1	61.7	6.8
234Flux	70.5	1.4	36.3	6.6
235Amor	49.4	5.7	38.5	2.5
282WCr	62.1	1.4	58.2	7.0
283HEA	63.4	4.1	61.3	7.6

Substrate A (34CrNiMo6) specimens showed the best tensile stress values. All tests, except for 235Amor samples, showed comparable tensile stress values. The 234FLux coating on substrate A was found to be the best in terms of maximum tensile stress.

2.1.2.3 Scratch Test (CSM/RINA)

RINA-CSM performed scratch test according to UNI EN ISO 2409 on coated samples listed below:

- High phosphorus undercoat, low phosphorus top coat (as plated, heat treated at 250C for 10 hours, heat treated at 300C for 2 hours)
- High phosphorus undercoat, high phosphorus top coat (as plated, heat treated at 250C for 10 hours, heat treated at 300C for 2 hours)
- Graphenea Xylan coating (reference)

This test method covers the determination of the resistance of coatings to separation from substrates when a right-angle lattice pattern is cut into the coating using a specific blade tool, penetrating through to the substrate. The property measured by this empirical test procedure depends, among other factors, on the adhesion of the coating to either the preceding coat or the substrate. This procedure is not to be regarded, however, as a means of measuring adhesion.

In Table 2.1.4 a six-step classification is given. The first three steps are satisfactory for general purposes and are to be used when a pass/fail assessment is required. Special circumstances can arise, in which case the complete six-step classification will be necessary.

Table 2.1.4 - Classification of test results

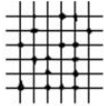



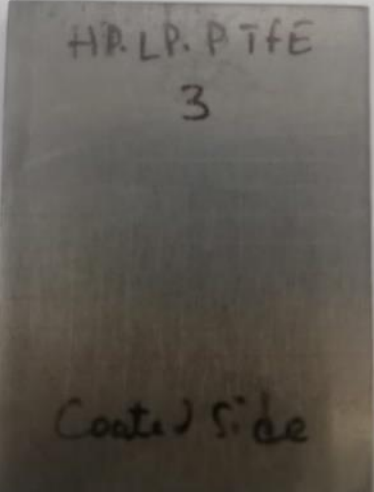
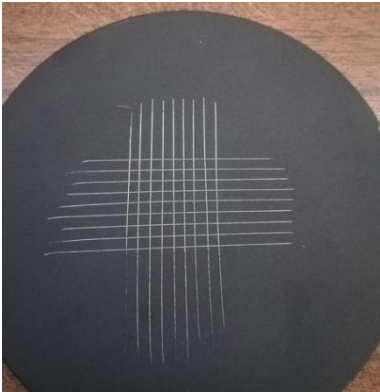
Classification	Description	Appearance of surface of cross-cut area from which flaking has occurred (Example for six parallel cuts)
0	The edges of the cuts are completely smooth; none of the squares of the lattice is detached.	—
1	Detachment of small flakes of the coating at the intersections of the cuts. A cross-cut area not greater than 5 % is affected.	
2	The coating has flaked along the edges and/or at the intersections of the cuts. A cross-cut area greater than 5 %, but not greater than 15 %, is affected.	
3	The coating has flaked along the edges of the cuts partly or wholly in large ribbons, and/or it has flaked partly or wholly on different parts of the squares. A cross-cut area greater than 15 %, but not greater than 35 %, is affected.	
4	The coating has flaked along the edges of the cuts in large ribbons and/or some squares have detached partly or wholly. A cross-cut area greater than 35 %, but not greater than 65 %, is affected.	
5	Any degree of flaking that cannot even be classified by classification 4.	—

Table 2.1.5 summarizes the results of the tests and the related images of the tested specimens. All samples but one resulted to have a perfect adhesion (Grade 0) according to the test procedure. Only the HP-HP-PTFE sample named in Table “AS PLATED HP HP PTFE (4)” resulted to have a Grade 2 adhesion which is acceptable.

Table 2.1.5 – Scratch test results

Sample	Figure	Classification
HP HP PTFE 250°C	 A photograph of a rectangular sample card with a light-colored, slightly textured surface. The card is oriented vertically. Handwritten in black ink at the top is "HP. HP. PTFE 2". Below that, further down, is "Coated side".	Grade 0
AS PLATED HP HP PTFE (4)	 A photograph of a rectangular sample card, similar to the first one. Handwritten in black ink at the top is "HP. HP. PTFE 4". Below that is "Coated side".	Grade 2
HP HP PTFE 300°C (6)	 A photograph of a rectangular sample card. Handwritten in black ink at the top is "HP. HP. PTFE 6". Below that is "Coated side".	Grade 0

HP LP PTFE 250°C (2)		Grade 0
HP LP PTFE 300°C (3)		Grade 0
HP LP PTFE (6)		Grade 0

<p>Graphenea Reference</p>	<p>Xylan</p> 	<p>Grade 0</p>
-----------------------------------	---	----------------

2.1.2.4 Slurry test (CSM/RINA)

CSM/RINA performed Slurry Test according to ASTM G75 standards to evaluate the response to the abrasivity of a specific mud for the different coatings developed during the previous phases of this project. The equipment used during tests is a Miller Machine, Figure 2.1.15.



Figure 2.1.15 - RINA Miller Number Machine

The duration of each test is 6 hours, specimen’s weight was measured every 2 hours of testing. Four samples were evaluated for each type of coating.

Tested samples received from TWI are listed in Table 2.1.6. Figure 2.1.16 to Figure 2.1.21 show the as received specimens.

Table 2.1.6 – Samples ID and Coating

ID	Coating Powder
232WC_A3	WC10Co4Cr
233CrC_A3	CrC-NiCr
234Flux_A3	Self Fluxing NiCrFeBSi
235Amor_A3	Nano-crystalline (C3Cr25B5Mo20Mn5Si2W10Fe)
282WCr_A3	Cermet WC-CrC-Ni
283HEA_A3	CoCrFeNiMo0.85 (HEA)

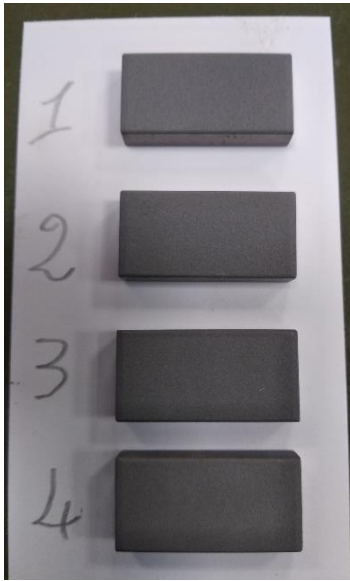


Figure 2.1.16 – 232WC_A3

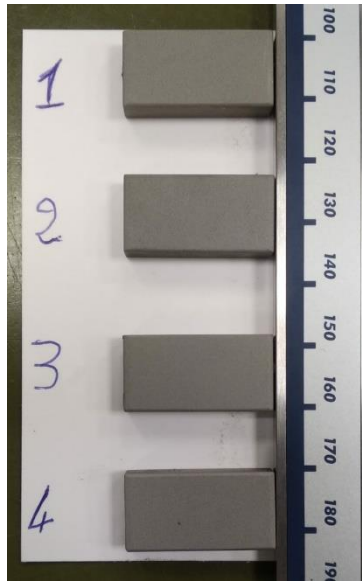


Figure 2.1.17 – 233CrC_A3

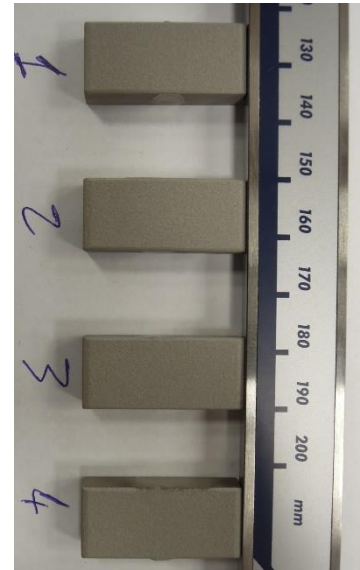


Figure 2.1.18 - 234Flux_A3

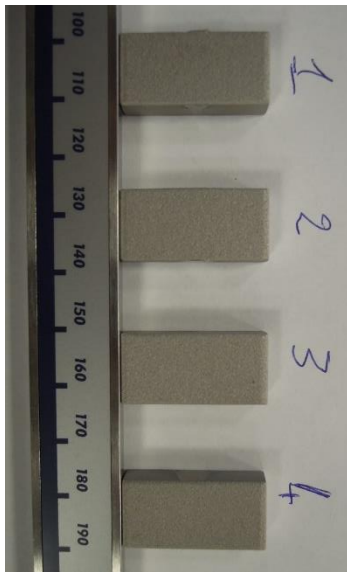


Figure 2.1.19 - 235Amor_A3

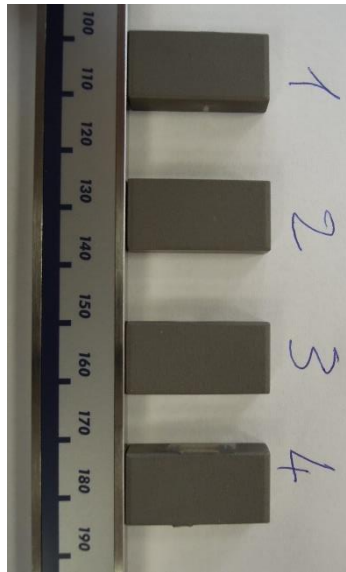


Figure 2.1.20 - 282WCr_A3



Figure 2.1.21 - 283HEA_A3

Slurry used during tests is composed of a liquid and a solid part expecting the following components:

- 60% Liquid phase (Clear Bore Polymer diluted with water and Sodium carbonate added as required to reach pH 9)
- 20% Gravel (Gravel Size: 2-3mm)
- 20% Sand (Sand Size: 10:18 0.85-1.7mm)

Weight losses have been considered as output of tests and starting from these the volume losses have been be calculated.

Figure 2.1.22 shows the cumulative average weight loss for every sample. Table 2.1.7 contains weight loss value for every 2h test step and a representative picture of the wear occurred to the samples.

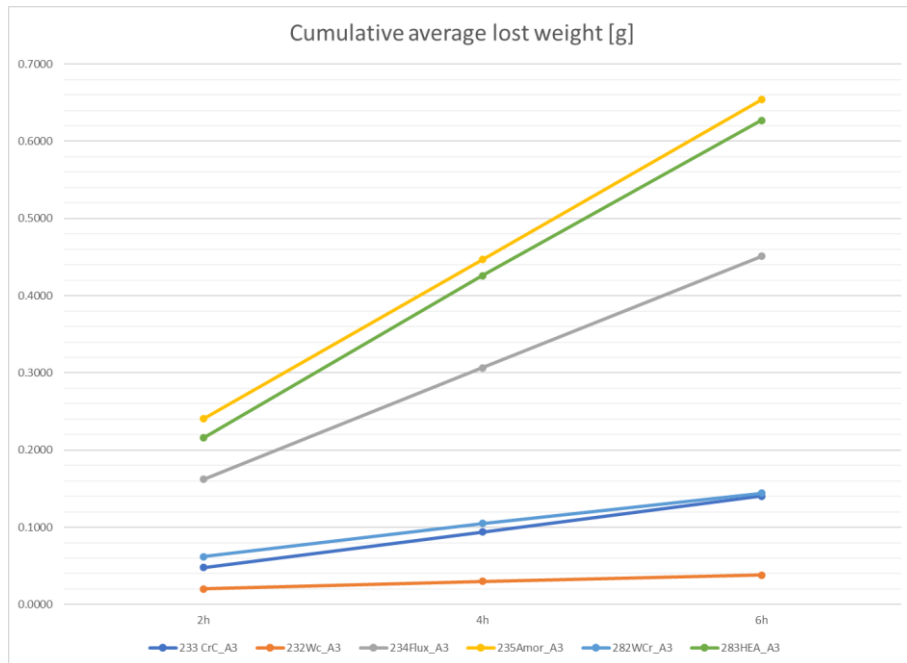


Figure 2.1.22 - Cumulative average weight loss [g] vs test time [h]

Table 2.1.8 - Cumulative weight loss [g]





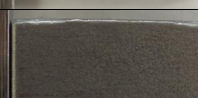

	AVERAGE LOST WEIGHT SUM [g]			Sample after 6h
	2h [g]	4h [g]	6h [g]	
232Wc_A3	0.0201	0.0301	0.0382	
233 CrC_A3	0.0478	0.0938	0.1402	
234Flux_A3	0.1621	0.3066	0.4509	
235Amor_A3	0.2406	0.4467	0.6540	
282WCr_A3	0.0620	0.1050	0.1443	
283HEA_A3	0.2158	0.4258	0.6269	

Figure 2.1.23 shows the cumulative average lost volume for every sample. Table 2.1.9 contains volume loss values for every 2h test step and a representative picture of the wear occurred to the samples.

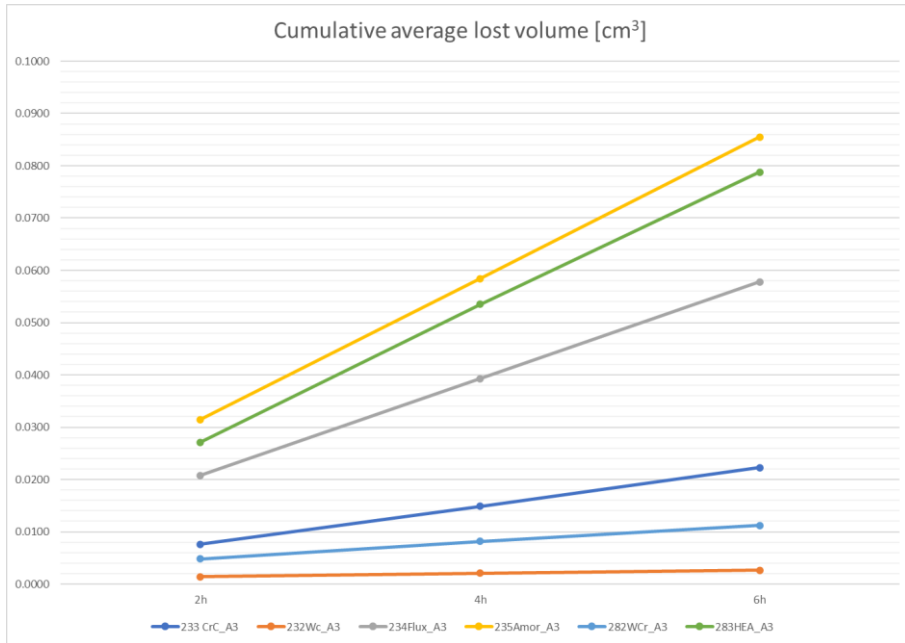


Figure 2.1.24 - Cumulative average lost volume [cm³] vs test time [h]

Table 2.1.10 - Cumulative volume loss [cm³]

	AVERAGE LOST VOLUME SUM [cm3]			Sample after 6h
	2h [cm3]	4h [cm3]	6h [cm3]	
232Wc_A3	0.0014	0.0021	0.0026	
233 CrC_A3	0.0076	0.0149	0.0222	
234Flux_A3	0.0208	0.0393	0.0578	
235Amor_A3	0.0314	0.0584	0.0855	
282WCr_A3	0.0048	0.0081	0.0112	
283HEA_A3	0.0271	0.0535	0.0788	

In this type of test, both the low value of weight loss (with associated loss in volume value) and the slope of the curve of the loss in weight (or volume) are important. The best result was obtained for the 232WC specimens.

The 233CrC and 282WCr specimens showed very similar weight (or volume) loss values, but the slope of the curves relating to the 282WCr specimens is lower than that of the 233CrC specimens.

2.1.3 Tribological test results

2.1.3.1 Pin-on-Disk dry rotating test at RT (Uol)

From Pin-on-disc dry rotating test carried out at RT:

- The friction coefficient results correlated with the wear resistance with the lowest values for the 0.5wt% GO and the reference neat Xylan coating for the rotational dry sliding test at RT. It is thus concluded that smaller addition of GO, i.e. 0.5wt% GO improved the dry sliding properties of the Xylan coating.
- The wear performance of all the ENP coatings was better than the Geo-Drill A5 substrate (34CrNiMo6); with lower wear rates. The HP-LP-PTFE 300 coating had the lowest wear rate of all the ENP coatings and all the low phosphorus coatings had lower Coefficient of Friction (CoF) and wear rates than the HP coatings. The HP-HP-PTFE 300 had the best performance of the high phosphorus coatings.
- The HVOF sprayed cermet based coatings 232WC, 233WC, and 282WCr had the highest wear resistance among the HVOF coatings tested in the PoD test under dry sliding conditions. The improved performance of the cermet coatings was displayed by non-measurable wear. The 232WC, 233CrC and 282WC were not penetrated, resulting in low material removal along the sliding interface. The worn volume and wear rate values of the counter ball (Al₂O₃ ball) was used to rank the coatings. The wear resistance is attributed to the carbide phases present in the coating. In general, the HVOF deposited cermet coatings exhibited excellent performance by abrasive wear out of the counter body Al₂O₃ ball.

Based on the results from the microstructural, mechanical, and dry PoD sliding test the 1-3 best performing coatings per coating group were selected for further testing at high temperature and tribo-corrosion sliding tests. The Xylan+0.5wt% GO coating was chosen from the Xylan-GO coating group and the heat treated ENPs (at 300°C); HP-HP-PTFE 300 and HP-LP-PTFE 300. The HVOF coatings selected for further tests were the 233WC, 234Flux and 282WCr coatings. The following sections describe the main results of the following tests:

2.1.3.2 Pin-on-Disk wet rotating test at 80°C (Uol)

From Pin-on-Disk wet rotating test at 80°C:

- The results showed a higher wear rate in the 0.5wt%GO during the 80°C wet sliding test compared to 0wt%GO but slightly lower CoF value was obtained for the 0.5wt%GO. This reduction in CoF can possibly be attributed to the GO sheets in the coating.
- The results from the PoD rotating wear test in water at 80°C of the down-selected HVOF coatings showed that when the load was increased to 30N in the 80°C test, considerable material removal was observed for the 233WC and 234Flux thus the wear volume and wear rate could be determined. Contrary to the dry sliding results, the coating with the best wear performance in the 80°C wet sliding test was 282WCr compared to the other down-selected coatings and the Geo-Drill substrate.
- The results obtained correlated closely to the room temperature dry sliding test, i.e. the HP-LP-PTFE 300 has lower wear rate for both tests. There is a clear drop in the measured average wear rates of the samples tested in the wet 80°C compared to the dry RT test. The lower values in the 80°C test are likely caused by the water minimizing the contact stresses by serving as a lubricant film between the coating and the Al₂O₃ ball.

2.1.3.3 Reciprocated sliding test at RT and 340°C (CSM/RINA)

CSM/RINA performed reciprocated alternating sliding tests in a non-lubricated regime on the samples listed in Table 2.1.11. During this test a pin slides alternately on the surface of the specimen to be tested with a certain frequency and a certain stroke. The pin is subjected to a force which ensures contact between it and the surface to be tested.

Table 2.1.11 – List of samples tested in reciprocated sliding test at RT and 340°C

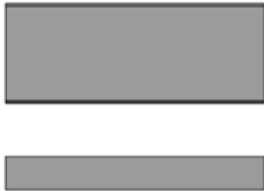
ID	Powder	Geometry
A10	Substrate Only 34CrNiMo6 (EN24T)	
232WC_A10	WC10Co4Cr	
282WCr_A10	Cermet WC-CrC-Ni	
HP.LP.PTFE 300°C		

Figure 2.1.25 shows the CETR UMT tribometer used during tests while Figure 2.1.26 shows the test layout

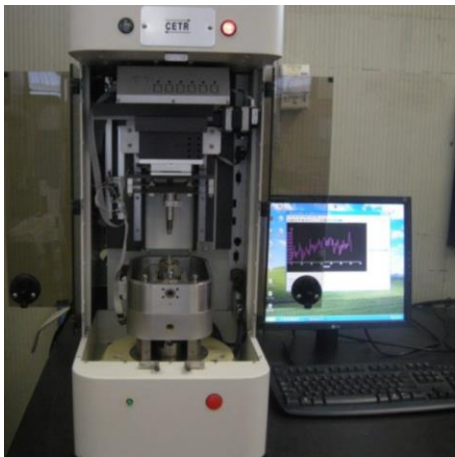


Figure 2.1.25 - CETR UMT Tribometer

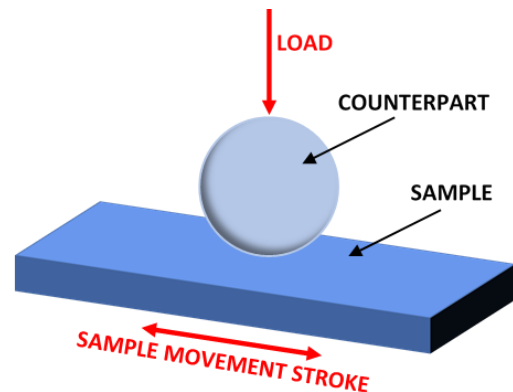


Figure 2.1.26 - Reciprocating sliding test scheme

The results of reciprocated sliding tests carried out by RINA are listed below.

Set parameters 1 tests results are listed in Table 2.1.1. Figure 2.1.27 and Figure 2.1.28 show the histograms of the results obtained.

Table 2.1.12 – Test parameters set 1 results

Sample	A10			232 WC			282WCr		
	Weight Loss Sample(g)	-0.0002	-0.0006	0.0001	-0.0084	-0.0046	-0.0082	-0.0021	-0.0023
Average Wight Loss Sample (g)	-0.0002			-0.0071			-0.0020		
Weight Loss Counterpart(g)	0.0003	-0.0001	-0.0001	-0.0006	-0.0003	0	-0.0001	-0.0006	0
Average Weight loss Counterpart (g)	0			-0.0003			-0.0002		
CoF	1.03	0.60	0.72	0.96	0.84	0.92	1.05	0.85	0.85
Average CoF SET 1	0.78			0.91			0.92		

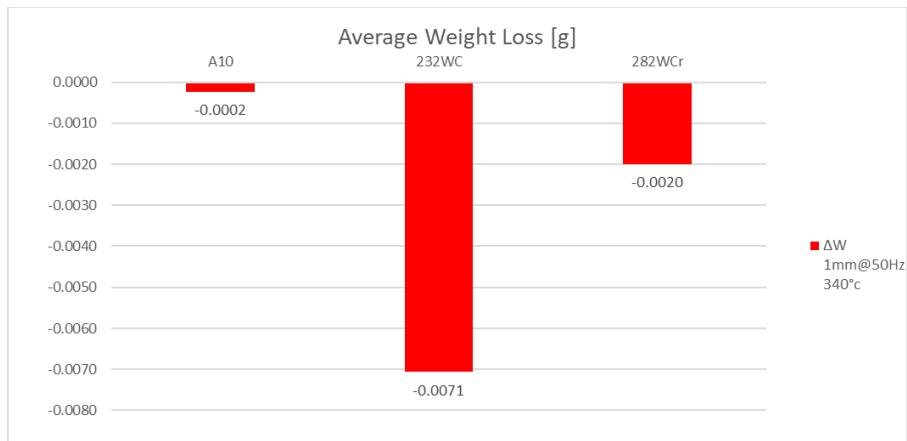


Figure 2.1.27 – Average weight loss for samples tested using Set parameter 1

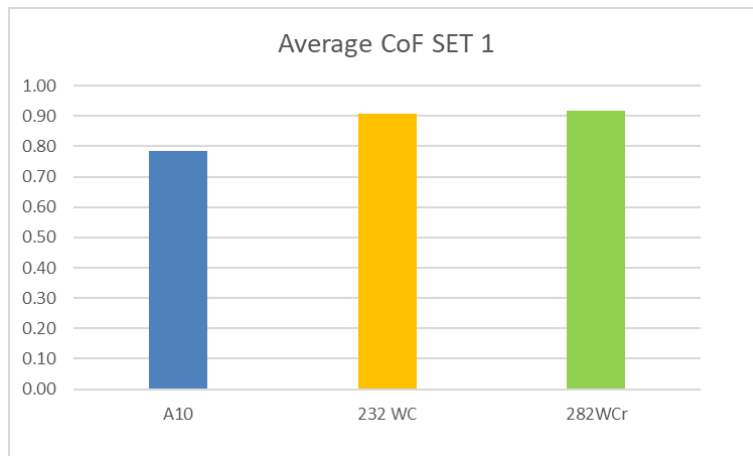


Figure 2.1.28 – Average coefficient of friction for samples tested using Set parameter 1

Set parameters 2 tests results are listed in Table 2.1.13. Figure 2.1.29 and Figure 2.1.30 show the histograms of the results obtained.

Table 2.1.13 - Test parameters set 2 results

Sample	A10		232 WC			282 WCr		
Weight Loss Sample(g)	-0.0005	-0.0010	-0.0042	-0.0046	-0.0023	-0.0011	-0.0019	-0.0047
Average Wight Loss Sample (g)	-0.0008		-0.0037			-0.0026		
Weight Loss Counterpart(g)	0	-0.0002	-0.0002	0	0	0	0	0
Average Weight loss Counterpart (g)	-0.0001		-0.0001			0		
CoF	0.88	0.81	1.13	0.99	1.08	1.10	0.99	1.11
Average CoF SET 2	0.85		1.07			1.07		

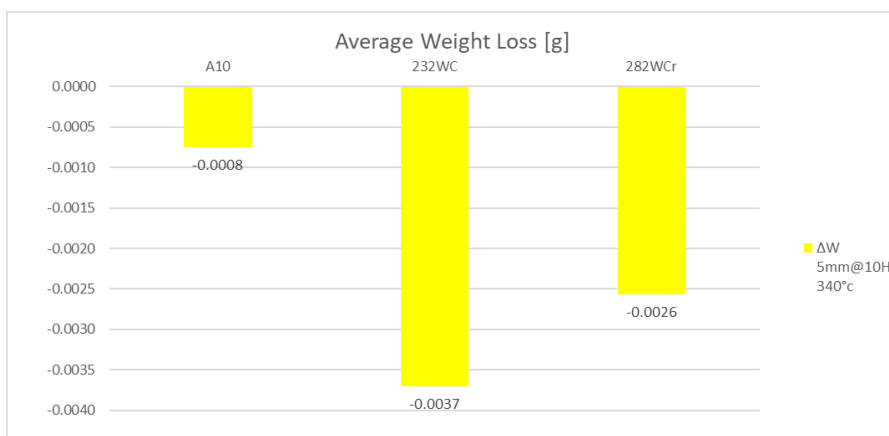


Figure 2.1.29 – Average weight loss for samples tested using Set parameter 2

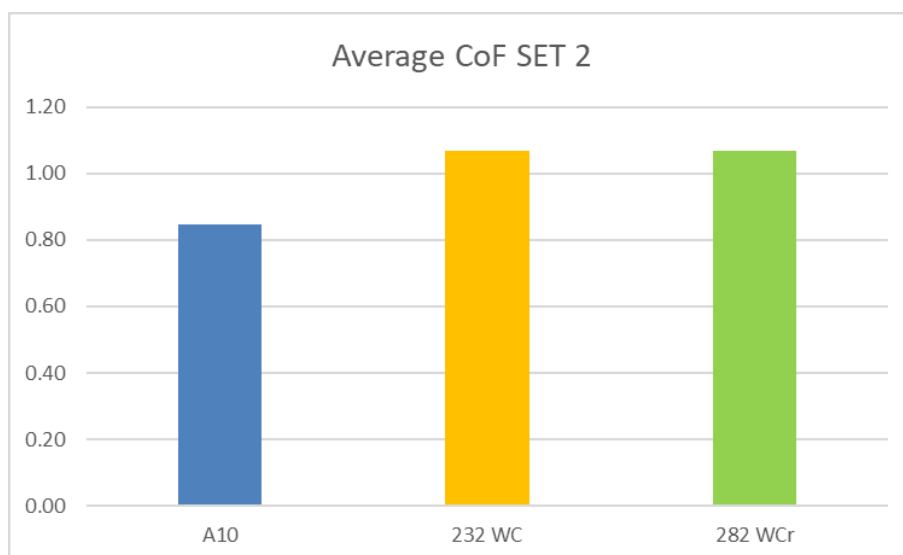


Figure 2.1.30 - Average coefficient of friction for samples tested using Set parameter 2

Set parameters 3 tests results are listed in Table 2.1.14. Figure 2.1.31 and Figure 2.1.32 Figure 2.1.29 show the histograms of the results obtained.

Table 2.1.14 - Test parameters set 3 results

Sample	A10		232 WC			282 WCr		
Weight Loss Sample(g)	-0.0007	-0.0016	-0.0028	-0.0018	-0.0010	-0.0002	-0.0004	-0.0010
Average Wight Loss Sample (g)	-0.0012		-0.0019			-0.0005		
Weight Loss Counterpart(g)	0	0	0	0.0001	-0.0001	-0.0003	0	-0.0001
Average Weight loss Counterpart (g)	0		0			-0.0001		
CoF	0.87	0.99	0.91	1.1	0.73	0.84	0.83	0.9
Average CoF SET 3	0.93		0.91			0.86		

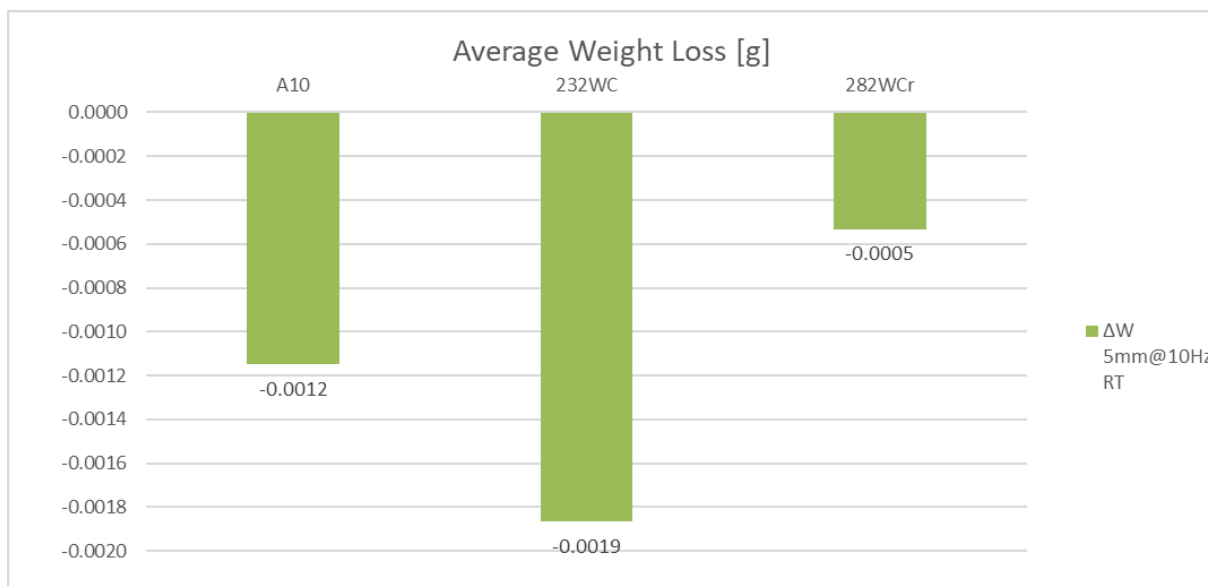


Figure 2.1.31 – Average weight loss for samples tested using Set parameter 3

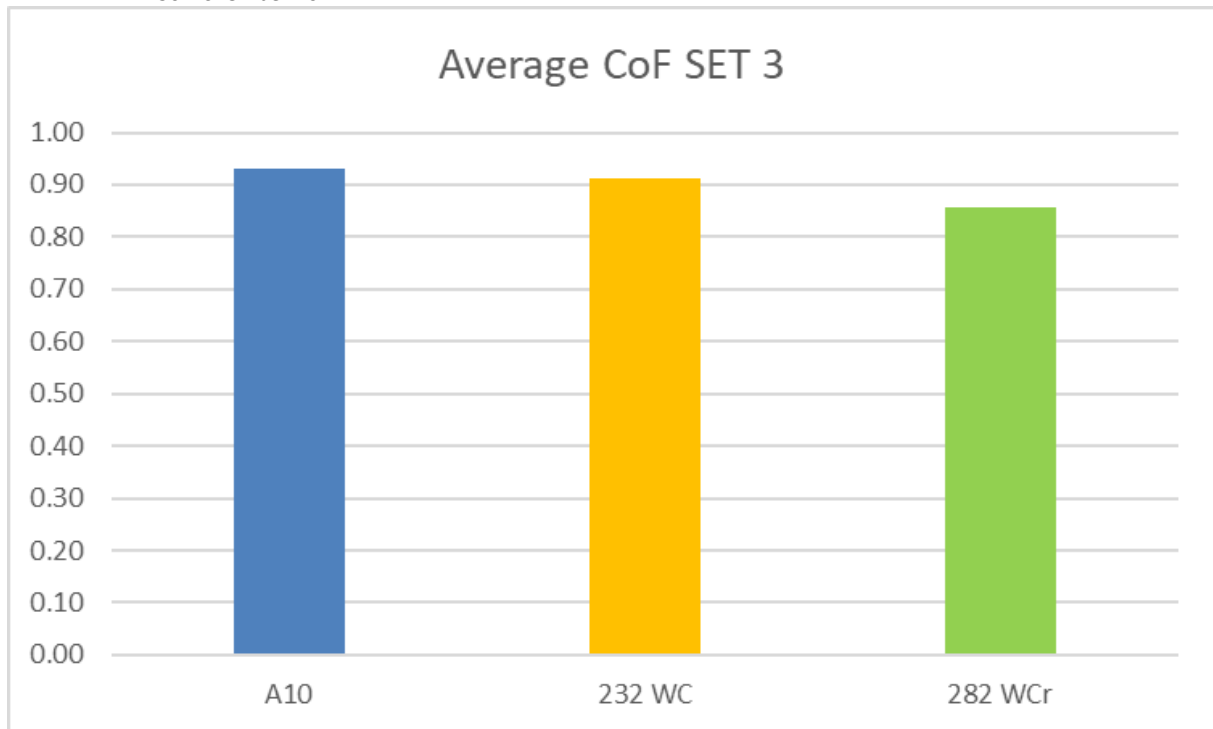


Figure 2.1.32 - Average coefficient of friction for samples tested using Set parameter 3

Wear rate were calculated using data relating to weight losses and density values shared with partners. Results for calculation are listed in Table 2.1.15.

Table 2.1.15 – Sliding test results for the different test set parameters

Set parameter 1 test		
Sample	Weight loss [g]	Wear Rate [mm ³ /Nm]
232WC	-0.0071	-0.00027
282WCr	-0.0020	-0.00009
A10	-0.0002	-0.00001
Set parameter 2 test		
Sample	Weight loss [g]	Wear Rate [mm ³ /Nm]
232WC	-0.0037	-0.00014
282WCr	-0.0026	-0.00011
A10	-0.0008	-0.00006
Set parameter 3 test		
Sample	Weight loss [g]	Wear Rate [mm ³ /Nm]
232WC	-0.0019	-0.00007
282WCr	-0.0005	-0.00002
A10	-0.0012	-0.00009

Table 2.1.16 resumes the results for specimens coated using HPLPPTFE300.

Table 2.1.16 – HPLPPTFE coated specimens test results

	HP LP PTFE	
Weight Loss Sample(g)	-0.0002	-0.0003
Average Wight Loss Sample (g)	-0.0003	
Weight Loss Counterpart(g)	-0.0001	0.0001
Average Weight loss Counterpart (g)	0.0000	
CoF	0.81	0.78
Average CoF SET 3	0.80	

The results obtained were found to be closely related to the test conditions. Even though the variations in terms of weight or volume during the test is measurable the values obtained are very low, meaning that substrate and coating tested have a good behaviour in the conditions of the test. Anyway, for tests at a temperature of

340 °C, we can observe that the coated specimens suffered greater weight losses than the uncoated specimens. The volume losses are much lower for the uncoated specimen for sliding at 50Hz and 1 mm of stroke, while they are comparable for sliding at 10Hz and 5 mm of stroke. For tests at room temperature, the 282WCr specimens showed less weight and volume loss than the uncoated specimens. According to these results the choice to use a coating on a specific component should be linked to the frequency of the load with which it is stressed and to the temperature of use.

2.1.3.4 Block-on-Ring test, RT & 650°C (CSM/RINA)

RINA performed Block on Ring (BoR) test at room temperature on the coated ring samples listed in Table 2.1.17 and at 650°C on the coated ring samples listed in Table 2.1.18 using the configuration shown in Figure 2.1.33. This test method covers laboratory procedures for determining the resistance of materials to sliding wear. During this test a test block is loaded against a test ring that rotates at a given speed for a given number of revolutions.

Table 2.1.17 – List of samples for BoR test at RT

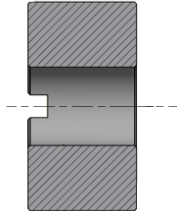
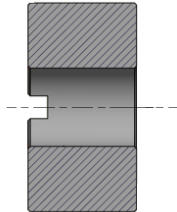
ID	Powder	Geometry
A11 highT (SUB)	Substrate Only 34CrNiMo6 (EN24T)	
232WC A11 lowT	WC10Co4Cr	
282WCr A11 lowT	Cermet WC-CrC-Ni	

Table 2.1.18 - List of samples for 650°C temperature BoR test

ID	Powder	Geometry
A11 highT (SUB)	Substrate Only 34CrNiMo6 (EN24T)	
234Flux A11 highT	Self Fluxing NiCrFeBSi	

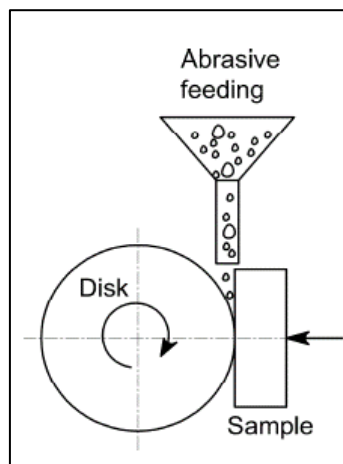


Figure 2.1.33 - BoR test configuration

The results of Block-on-Ring test carried out by RINA are listed below. Figure 2.1.34 shows the average weight loss recorder during room temperature tests. Figure 2.1.35 to Figure 2.1.42 show the samples after tests.



Figure 2.1.34 - Average weight loss for samples tested at R.T.

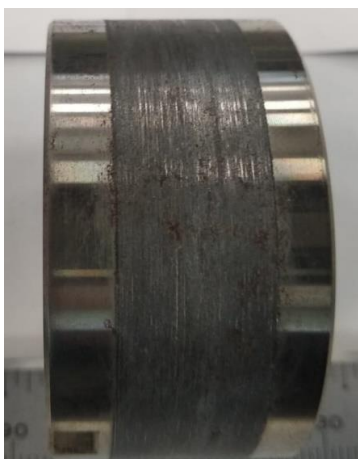


Figure 2.1.35 – A11 (-0.247 g)

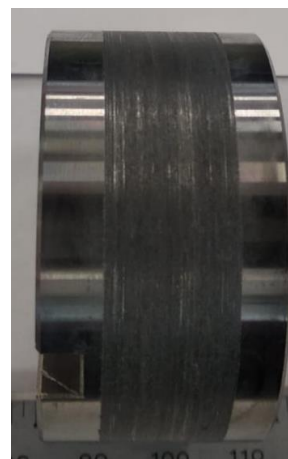


Figure 2.1.36 – A11 (-0.173 g)



Figure 2.1.37 - 232WC (-0.0810 g)



Figure 2.1.38 - 232WC (-0.0640 g)



Figure 2.1.39 - 232WC (-0.1180 g)

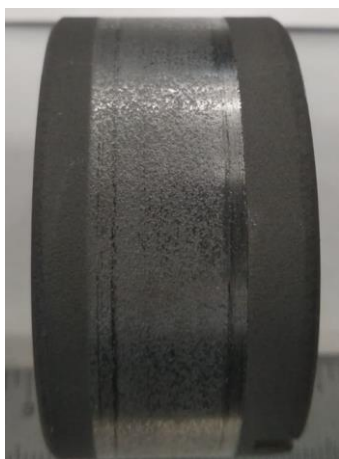


Figure 2.1.40 – 282WCr (-0.094 g)

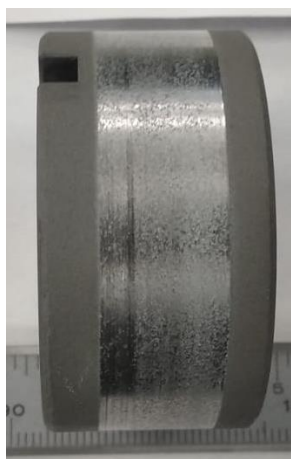


Figure 2.1.41 - 282WCr (-0.144)

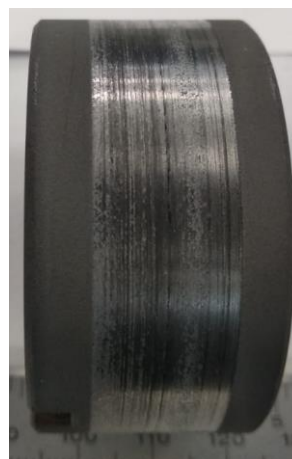


Figure 2.1.42 - 282WCr (-0.144)

Figure 2.1.43 shows the average weight loss recorded during high temperature tests. Figure 2.1.44 to Figure 2.1.48 show the samples after tests.

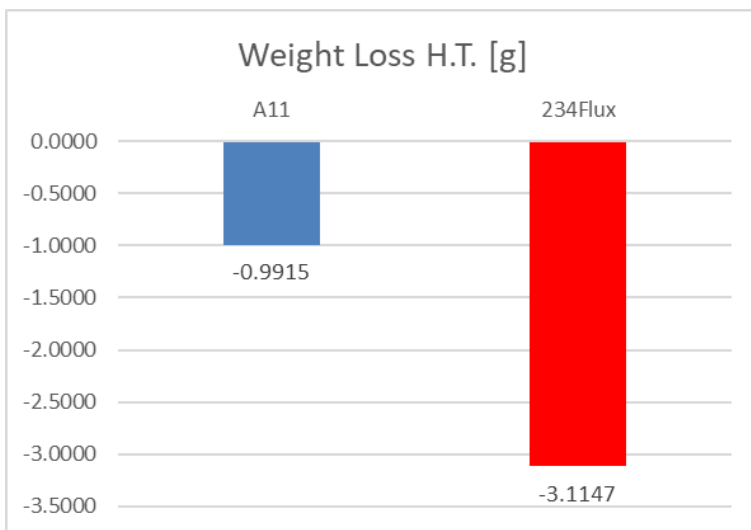


Figure 2.1.43 - Average weight loss for samples tested at High Temperature.



Figure 2.1.44 – A11 (-1.149 g)



Figure 2.1.45 – A11 (-0.8340 g)



Figure 2.1.46 – 234Flux (-2.1300 g)

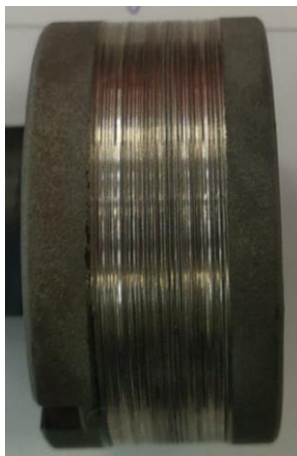


Figure 2.1.47 - 234Flux (-3.3580 g)

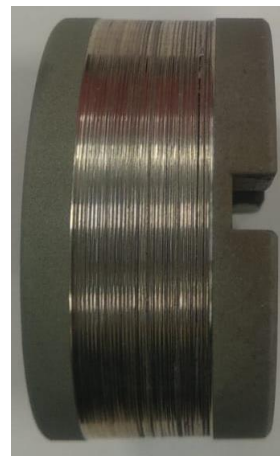


Figure 2.1.48 - 234Flux (-3.3850 g)

Wear rate were calculated using data relating to weight losses and density values shared with partners. Results for calculation are listed in Table 2.1.19.

Table 2.1.19 – Block on Ring test results for different temperatures tests

Room Temperature tests results		
Samples	Weight loss [g]	Wear Rate [mm ³ /Nm]
232WC	-0.0877	-0.00001
282WCr	-0.127	-0.00002
A11	-0.21	-0.00005
High Temperature tests results		
Samples	Weight loss [g]	Wear Rate [mm ³ /Nm]
234Flux	-3.1147	-0.00074
A11	-0.9915	-0.00023

Considering the tests at room temperature both coatings were found to be more effective than the substrate material. The 232WC coated sample was found to be the best in terms of wear resistance and volume loss. The wear surfaces of the 232WC specimens appear to be less prone to plowing than those of the 282WCr specimens. On the contrary, the surfaces of the uncoated specimens are affected by severe wear. High temperature tests have shown that the coating 234Flux is ineffective under this test conditions. The 234Flux specimens show signs of plowing when compared to the uncoated specimens.

2.1.3.5 Trobi-corrosion test in saline fluid at RT (UoI)

Based on the investigations, the following main conclusions are drawn:

- The results from the potentiodynamic polarization tests show a higher corrosion potential (E_{corr}) for the Xylan+0.5wt% GO compared to the neat Xylan (0wt% GO). This signifies higher corrosion resistance with the recorded low corrosion current density. The Xylan+0.5wt% GO also outperforms the neat Xylan (0wt% GO) after the combined corrosion and sliding test with lower wear volume measured and lower CoF.
- A short passive behavior characterized both 232WC and 282WCr with a decrease in passive current density to 10^{-4} A/cm². The smallest corrosion current was observed for the 234Flux. The 232WC, 282WCr and 234Flux had a better corrosion and friction coefficient values compared to the Geo-Drill A5 substrate. The coating with the best corrosion and friction and corrosion performance is 234Flux for the RT tribo-corrosion test in saline fluid. The corrosion properties was portrayed by the more positive Open Circuit Potential (OCP) values before sliding, after sliding and during recovery.
- There is no significant difference in the obtained corrosion potential (E_{corr}) for both ENP coatings. However, neither coating showed passive behaviour, nevertheless the resulting corrosion current measured was very low (10^{-8} A/cm²). From the corrosion test, a similar trend was observed for the corrosion and sliding test. However, stability in the friction coefficient in both coatings was low. A slightly lower drop in potential was observed for the HP-LP-PTFE300°C.

2.1.3.6 Tribo-corrosion test in NS4 solution at 80°C (CSM/RINA)

The tribo-electrochemical test apparatus used for the tribo-corrosion tests at elevated temperature (80°C) is a standard pin-on-disc (ball-on-disk) tribometer (RTM, Italy), having a modified configuration with a three-electrode electrochemical cell added. To ensure the electric insulation the electrochemical cell is made of a polymeric corrosion resistant material and the same for the polymeric ball-holder where the counterpart, namely a 10 mm diameter Al₂O₃ sphere (1120 HV), is clamped.

In the cell, the reference electrode is a saturated calomel (SCE) while the counter electrode is a Pt wire. The modified RTM ball-on-disk tribometer overview, and some details of the cell are shown in the two pictures reported in Figure 2.1.49.



Figure 2.1.49 - The modified RTM ball-on-disk tribometer (left) with the electrochemical cell during a test. Right some details of the cell. Bottom, Xylan disk for tribocorrosion test

The pin-on-disk test is a model test for determining friction and wear of two solid surfaces being in sliding contact, namely pin or ball against coated disk. The load is usually selected considering the application, the material, and the available testing system.

For tests above room temperature (RT) the testing apparatus is provided with a heating system to keep the solution at fixed and constant T value, by a coil that is located inside the cell, Figure 2.1.50.



Figure 2.1.50 - Detail of the heating system with the coil inside the cell

Specimens for the tribocorrosion tests at 80°C in NS4 fluid were provided by Graphenea (Xylan coatings) and TWI (substrates and Cermet HVOF coatings):

- Disks coated by Xylan and modified Xylan + 0.5 wt% GO.
- Disks CerMet coated: 282WCr, 232WC
- Steel disks (substrate): 34CrNiMo6
- C40 disks coated by Neat Xylan (a few specimens used for some preliminary tests only)

The testing fluid/solution, initially proposed for the activity was the liquid fraction of a drilling fluid used for tribological tests at CSM/RINA, consisting of the following:

- Clear Bore Polymer diluted with water to obtain a Marsh Funnel Viscosity of 60 seconds.
- Sodium carbonate added as required to reach pH 9.

Preliminary tests highlighted that this fluid was unsuitable for the electrochemical measurements, due to meaningless curves (shape, scattered points) and low electric signals obtained in corrosion experiments. As an alternative a synthetic soil NS4 solution/electrolyte was proposed for the present activity. This solution, originally proposed by Parkins [1], represents the average composition of the aqueous extract of the soils in which numerous cases of Near Neutral Stress Corrosion Cracking (NN-SCC - which is a particular form of stress corrosion cracking) take place on coated buried pipelines. The NS4 solution has pH equal to 8.3.

The solution, NS4, has the following chemical composition:

- KCl= 0.122 g/l
- NaHCO₃ = 0.483 g/l
- CaCl₂·2H₂O = 0.181 g/l
- MgSO₄·7H₂O = 0.131 g/l

A modified protocol with respect to the one used for tribocorrosion assessment, was adopted due to several interferences in the electrochemical measurements, evidenced during the preliminary tests on Xylan coatings, (possibly related to low currents, intrinsic nature of the material combined with the specific solution, temperature 80°C- solution evaporation).

In principle, potentiodynamic curves having irregular shape (and/or scattered points) are not suitable for the necessary elaboration to extract parameters of interest (fitting). Since interferences, as expected, were more intense during the rubbing steps but were consistently reduced when the rubbing (and the cell rotation) was stopped, it was decided to adjust the protocol accordingly. It is worth noting that the modified protocol aims at the evaluation of tribo and corrosive phenomena, to identify the effect of tribocorrosion on the material under study after the material has been worn out and simultaneously corroded, but not while those phenomena are taking place.

During sliding wear, CoF and tribocorrosion are characteristics for the material and the selected experimental conditions. The electrochemical curves are collected after the 'relaxation' time that is necessary to reach constant Open Circuit Potential (OCP) value, with motionless solution, as required by the method for the electrochemical measurements.

In summary, the material under study is first worn out and then analyzed by OCP/PD measurements. This is repeated for a certain number of steps, according to the material characteristics. The load value to be applied was defined in preliminary tests. The potential was scanned in a small range close to the detected equilibrium value (± 30 mV), where the current density is very small, and irreversible electrochemical reactions responsible of the degradation of the investigated material cannot take place. This allows the same specimen to be used for several times in multistep tests (Wear-CoF/OCP-PD).

Evaluation of the parameters of interest were carried out generally according to ASTM G99 (wear), ASTM G3 and ASTM G59. Tafel method was applied on polarization plots only when the analysis was possible, according to the curve quality.

Characterization methods (tested samples)

Tested specimens, Table 2.1.20, were investigated by:

- Weight variation, Δp (analytical scale Mettler-Toledo 0.1 mg readability)
- Optical Microscope (OM), to assess the coating adhesion, thickness and damage after tests (cross section) and surface quality (surface investigation).
- Scanning Electron Microscope (SEM JEOL 6480, EVO MA15) with EDS (INCA Oxford, EDAX) microanalysis. When necessary investigation was carried out on both cross section and specimen surface. By SEM/EDS surface and cross sections of specimens were characterized to better evaluate the damage occurred in the tested coatings and the morphological and chemical modifications.
- Profilometry: an initial investigation for the evaluation of the depth of was scars were carried out by Mitutoyo mod Sv 3100 H4.

Table 2.1.20 – Tested samples

ID	Material	Geometry
SUBSTRATE	34CrNiMo6 Steel	
232WC_CA1	WC10Co4Cr CerMet	
282WCr_CA3	WC-CrC-Ni CerMet	
Modified Xylan	Xylan + 0.5 wt% GO	
Xylan	Xylan+0 wt% GO	

Xylan and Xylan0.5wt%GO Coatings (34CrNiMo6 substrate)

After a series of preliminary tests, the selected normal load applied to the ball was fixed to 10 N. The normal load was applied for 3 cycles lasting 30 min each, with a rotational speed of 120 RPM on a sliding diameter path of 16 mm, corresponding to 0.1 m/s.

For specimens tested all the Open Circuit Potential (OCP) has a duration of 30 min and the potentiodynamic scan is conducted at 0.1667 mV/s.

Table 2.1.21 – Pin-on-disk and potential parameters used for Xylan and Xylan0.5wt%GO tests

Material	Load (N)	Speed (RPM)	Track diameter (mm)	Temperature (°C)	OCP (min)	PD (mV)
Xylan 0.5wt% GO	10	120	16	80	60	±30
Xylan	10	120	16	80	-	-
Xylan 0.5wt %GO	10	120	16	80	-	-
The total length for 90 min test (0.1 m/s) is 540 m						

HVOF Coatings and substrate

Tests on 34CrNiMo6 steel substrate and on coated specimen 232WC (CA1) and 282WCr (CA3). After a series of preliminary tests, the selected normal load applied to the ball was 100 N, applied for 2 cycles lasting 30 min each, at the beginning, with a rotational speed of 120 RPM (0.1 m/s). Then the test duration was doubled to reach 120 min. Since 30 min corresponds to a length of 180 m, the total length for 120 min is 720 m.

Table 2.1.22 - Pin-on-disk and potential parameters used for steel substrate and 232WC and 282WCr coated specimens

Material	Load (N)	Speed (RPM)	Track diameter (mm)	Temperature (°C)	OCP (min)	PD (mV)
34CrNiMo6	100	120	16	80	60	±30
232WC	100	120	16	80	60	±30
282WCr	100	120	16	80	60	±30
The total length for 120 min test (0.1 m/s) is 720 m						

Results for Xylan0.5wt%GO and Xylan coatings, NS4 @80°C: CoF

Xylan0.5wt%GO coatings were investigated in tribocorrosion tests at OCP with and without the electrochemical perturbation. Xylan specimens were investigated without any electrochemical perturbation. During sliding the friction coefficient was recorded.

Figure 2.1.51 summarizes the CoF of Xylan based coatings as average values for 60 minutes testing.

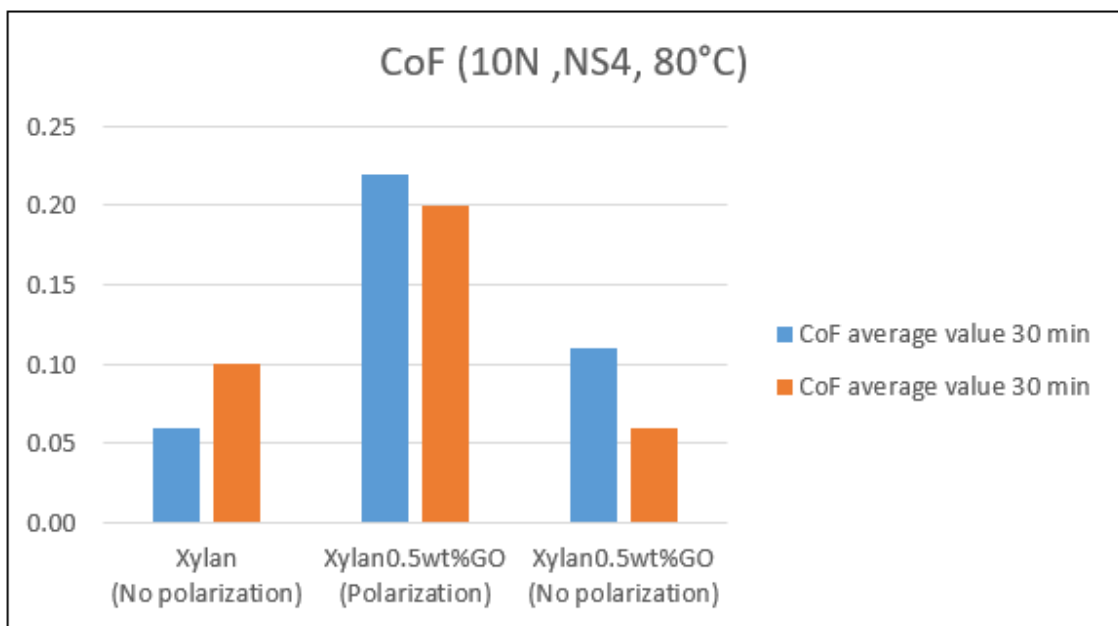


Figure 2.1.51 - CoF of Xylan based coatings as average values for 60 minutes testing.

As an example, Figure 2.1.52 shows a plot of the CoF for a single step.

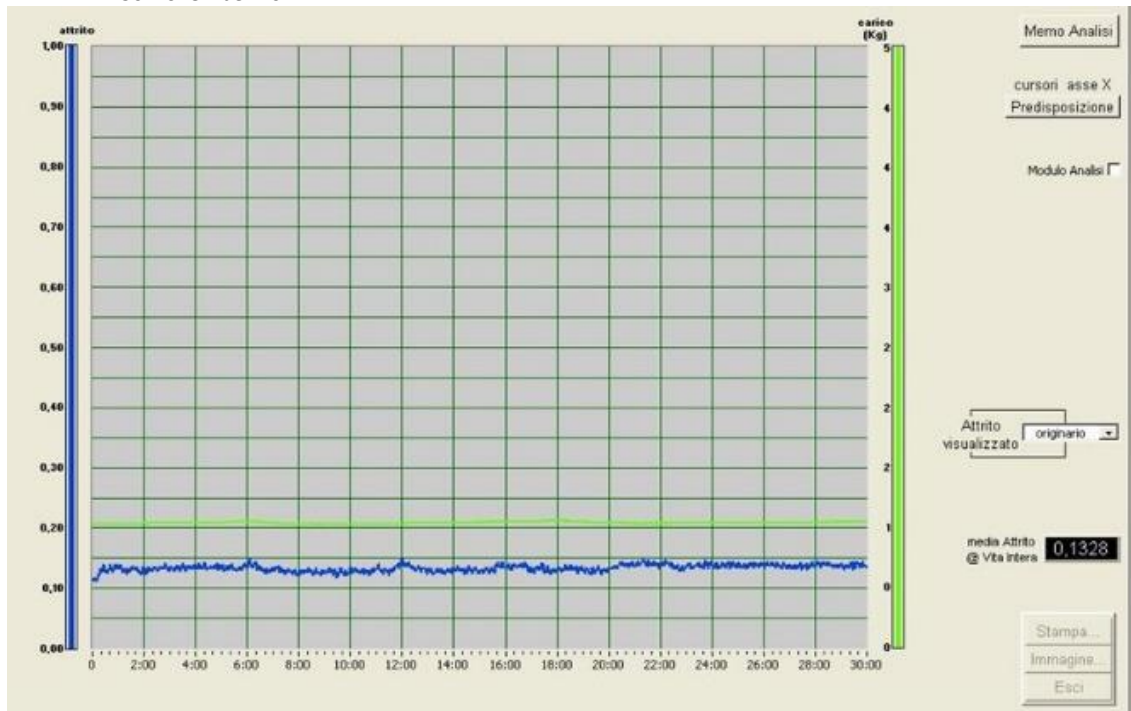


Figure 2.1.52 - One of the CoF plot reporting the curve for Xylan0.5wt %GO single wear step 30 min lasting (load in kg – y axis).

Results for Xylan0.5wtGO, NS4 @80°C: tribocorrosion

For the Xylan0.5wt%GO coatings the curves OCP (open circuit potential) and PD (potentiodynamic) concerning the multistep experiment are reported in Figure 2.1.53. Two modes of reporting of OCP plots are shown: the first one representing the E sequence as recorded vs time, the second one (3rd plot) the curves grouped and all starting at t=0.

As the coating is worn, E decreases toward the stabilization in the range between -0.3 < x < -0.2 V. Each three-step experiment (corresponding at 1h sliding wear) the sample was shortly investigated by profilometry to assess the extent of the damage in terms of track depth. This was quite difficult to achieve, since it seemed that the coating appeared almost unchanged with a minimal wear scar with respect to its initial thickness. This was not fully confirmed by SEM investigation at the end of the test.

The potentiodynamic curves shape looks quite irregular (parameters were not quantified) while a qualitative evaluation clearly show that they are grouped at two main positions in the plot with respect the current interval (their position in the diagram moves from point 1, representing the material in its original state before being worn out, to point 2 after 30 min wear at 10N and relaxation and, afterward, to lower current values).

It is worth noting a group of curves that is located at high current density (~ 10⁻⁵ - 10⁻⁴ A/cm²).

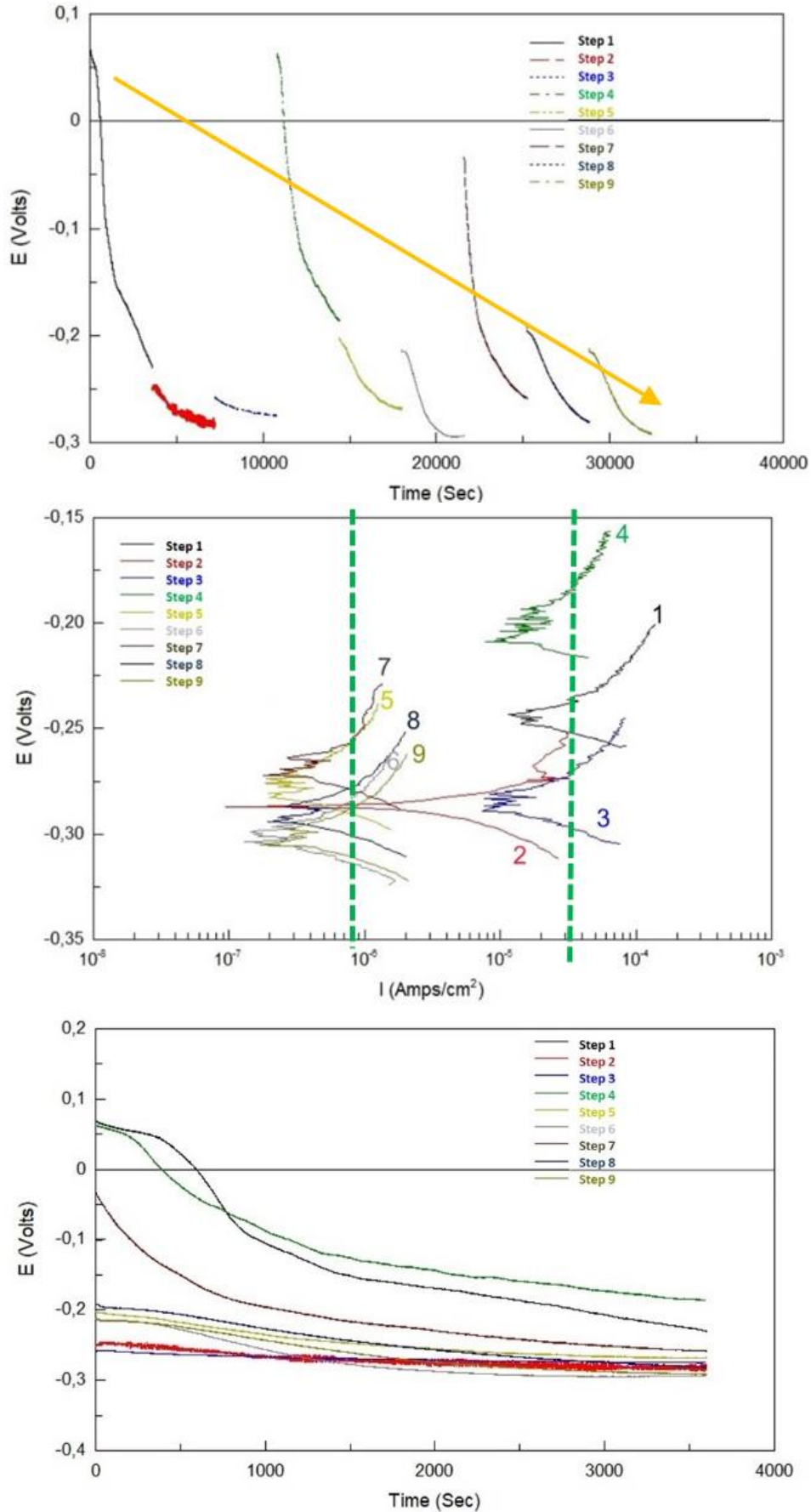


Figure 2.1.53 - Open circuit potential and potentiodynamic curves for one specimen of Xylan0.5wt%GO coating in a nine-step experiment of wear and corrosion carried out in NS4 solution @80°C temperature

OM analysis

After the immersion in the heated solution the material Xylan0.5wt%GO gradually modifies its appearance with the growth of some brown spots detected by OM Figure 2.1.54:

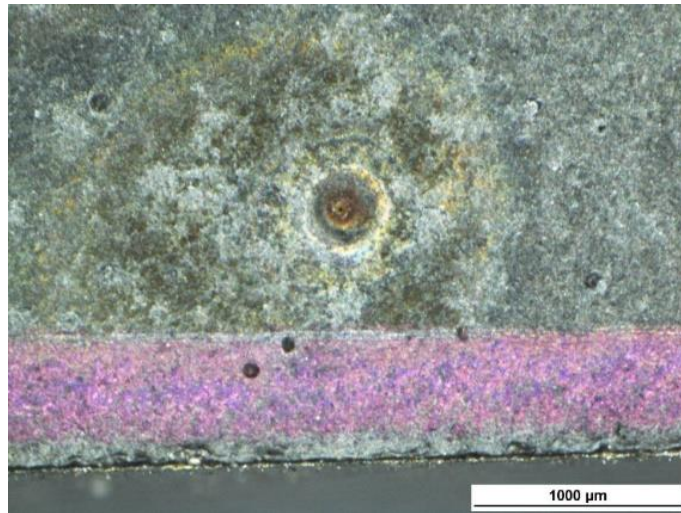


Figure 2.1.54 - OM image of the surface of Xylan0.5wt%GO coated specimen after the tribocorrosion test in NS4 solution @80°C. Large and small pores.

In Figure 2.1.55 the wear track of Xylan0.5wt%GO coated specimen after the 9-step tribocorrosion test.

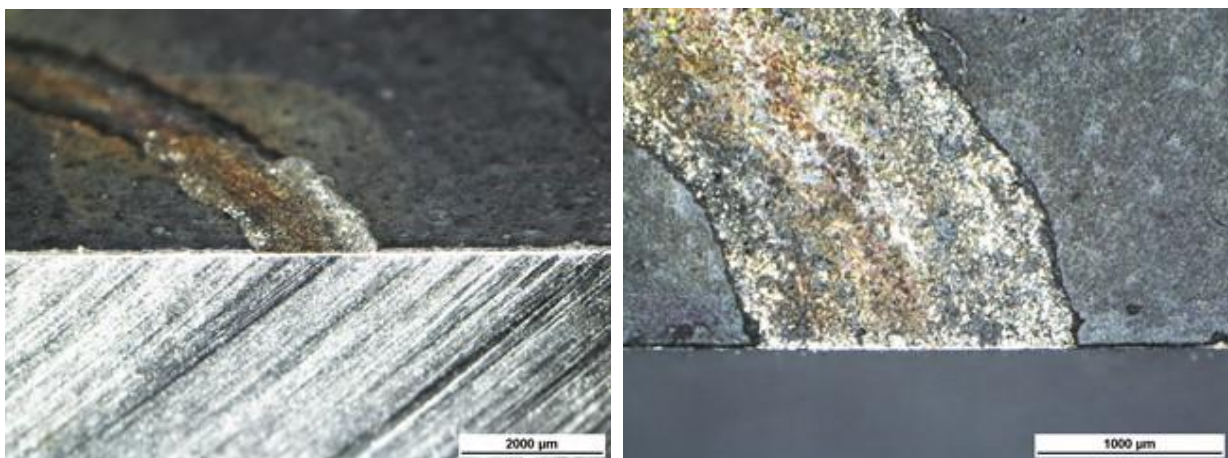


Figure 2.1.55 - OM images of the wear track for Xylan0.5wt%GO coating after the tribocorrosion test in NS4 solution @80°C (as cross-cutted)

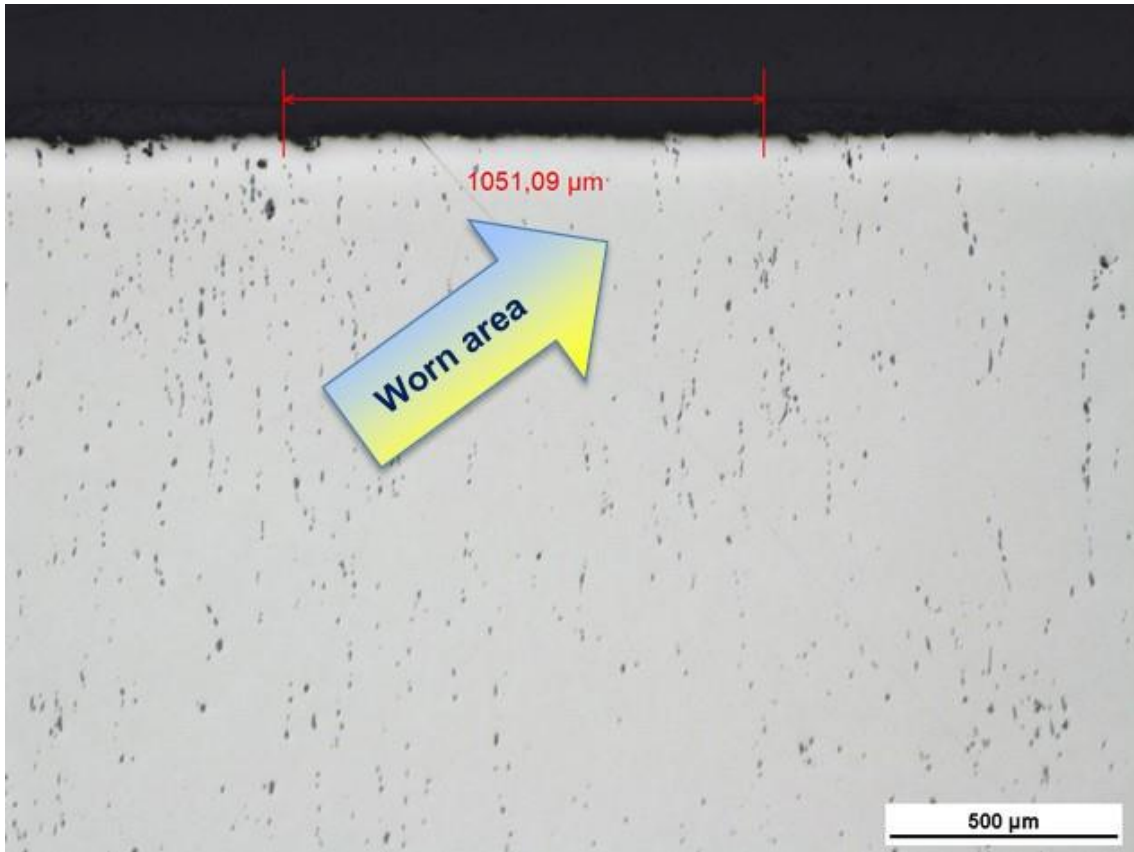


Figure 2.1.56 - OM image of the cross section for Xylan0.5wt%GO coated specimen after the tribocorrosion test in NS4 solution @80°C with the track zone identified by the arrow

SEM/EDS analysis

SEM investigation better evidenced the detachment of the coating that was completely removed in most of the wear track, or strongly reduced in its thickness; parts of the coating not detached show a fully porous structure with some large and deep porosities with exposed surface possibly with modified composition Figure 2.1.57:

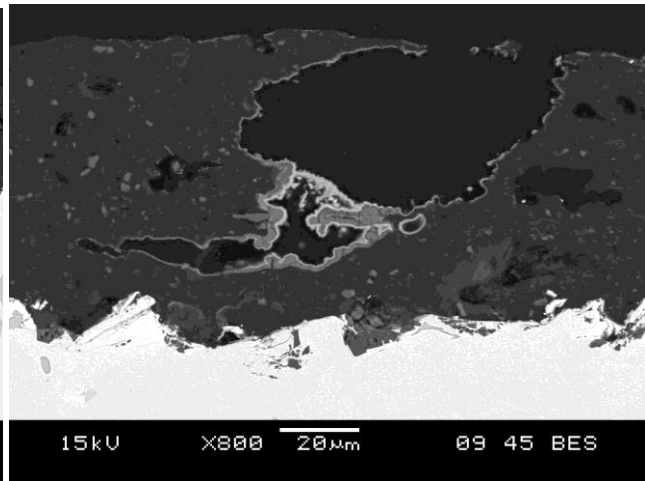
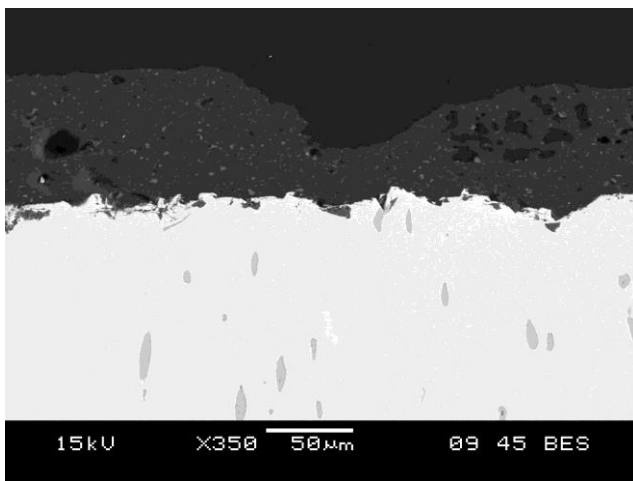
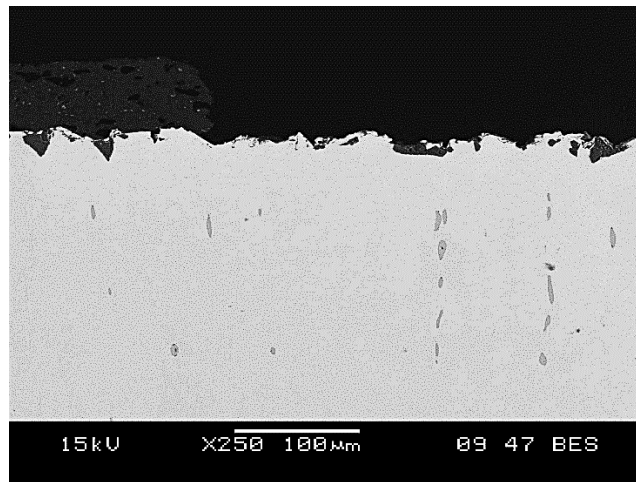
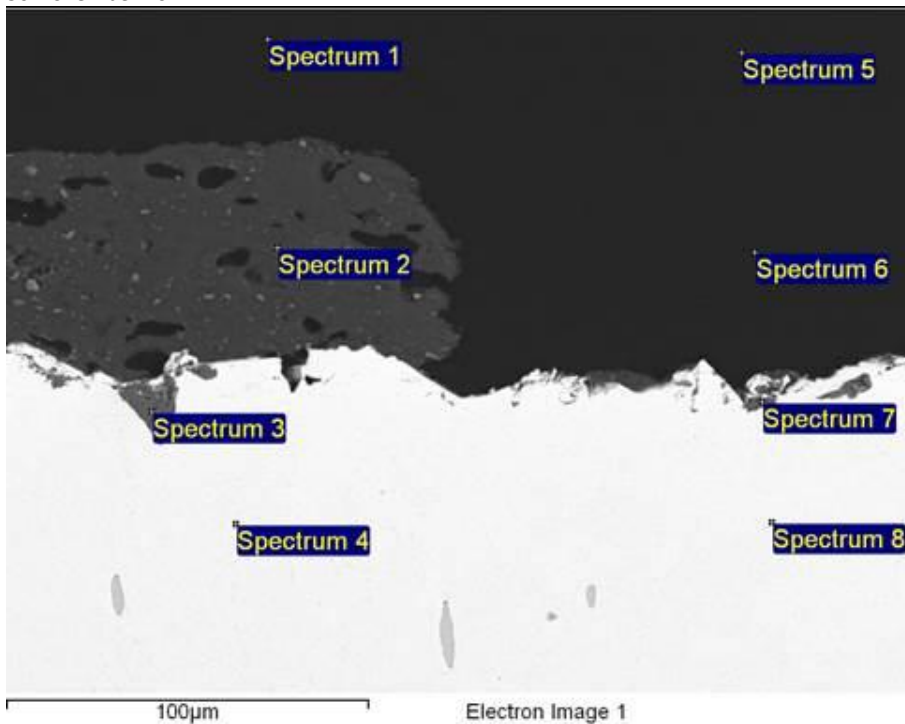


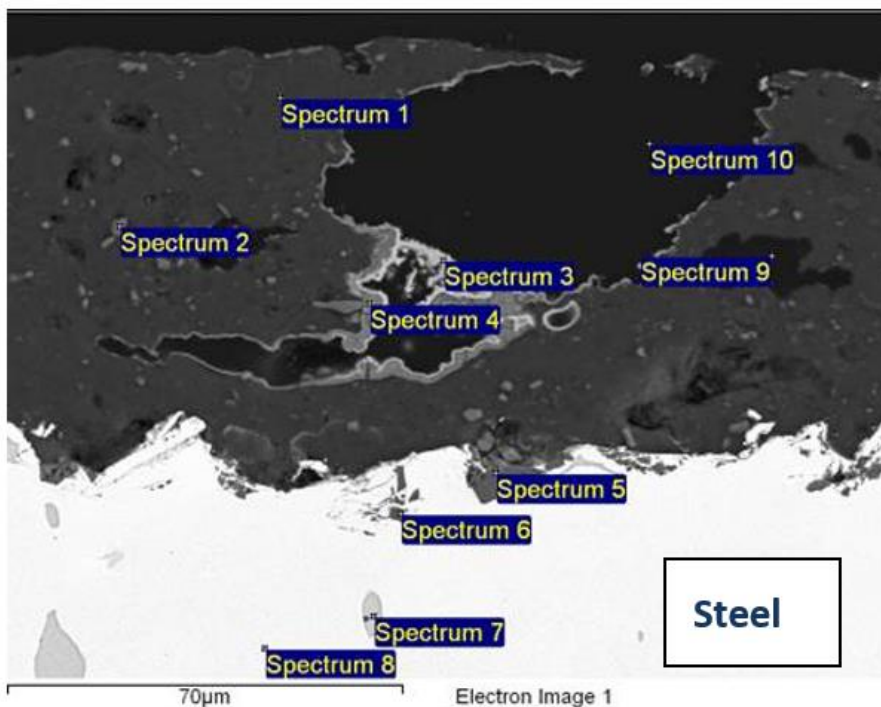
Figure 2.1.57 - SEM micrographs of the cross section for Xylan0.5wt%GO coated specimen after the tribocorrosion test in NS4 solution @80°C. Upper images: wear track zone with the coating completely detached. Lower images: wear track zone. Large and deep porosity deposited residuals. Backscattered mode (Mag. 250X, 350X, 800X).

The EDS elemental analyses, Figure 2.1.58, evidenced the presence of oxides:



Spectrum	In stats.	C % wt	O % wt	Al % wt	Si % wt	Cl % wt	Cr % wt	Mn % wt	Fe % wt	Mo % wt	Total % wt
1	Yes	85.19	11.67			3.15					100.00
2	Yes	50.25			0.54					49.22	100.00
3	Yes	10.96	38.18	50.87							100.00
4	Yes	7.01	1.01				17.14		74.84		100.00
5	Yes	93.94				6.06					100.00
6	Yes	86.88	10.16			2.96					100.00
7	Yes	17.38	35.23	42.57					1.91	2.92	100.00
8	Yes	6.60	1.18				17.16	1.00	74.05		100.00

Figure 2.1.58 - EDS point analysis for Xylan0.5wt%GO post-tribocorrosion test



Spectrum	In stats.	C % wt	O % wt	Al % wt	Si % wt	Cl %wt	Cr % wt	Mn % wt	Fe % wt	Mo % wt	Total %wt
1	Yes	85.19	11.67			3.15					100.00
2	Yes	50.25			0.54					49.22	100.00
3	Yes	10.96	38.18	50.87							100.00
4	Yes	7.01	1.01				17.14		74.84		100.00
5	Yes	93.94				6.06					100.00
6	Yes	86.88	10.16			2.96					100.00
7	Yes	17.38	35.23	42.57					1.91	2.92	100.00
8	Yes	6.60	1.18				17.16	1.00	74.05		100.00

Figure 2.1.59 - EDS point analysis for Xylan0.5wt%GO post-tribocorrosion test

Surface SEM/EDS investigation on post-tested coating clarified the nature of the spots identified by the naked eye, Figure 2.1.60.

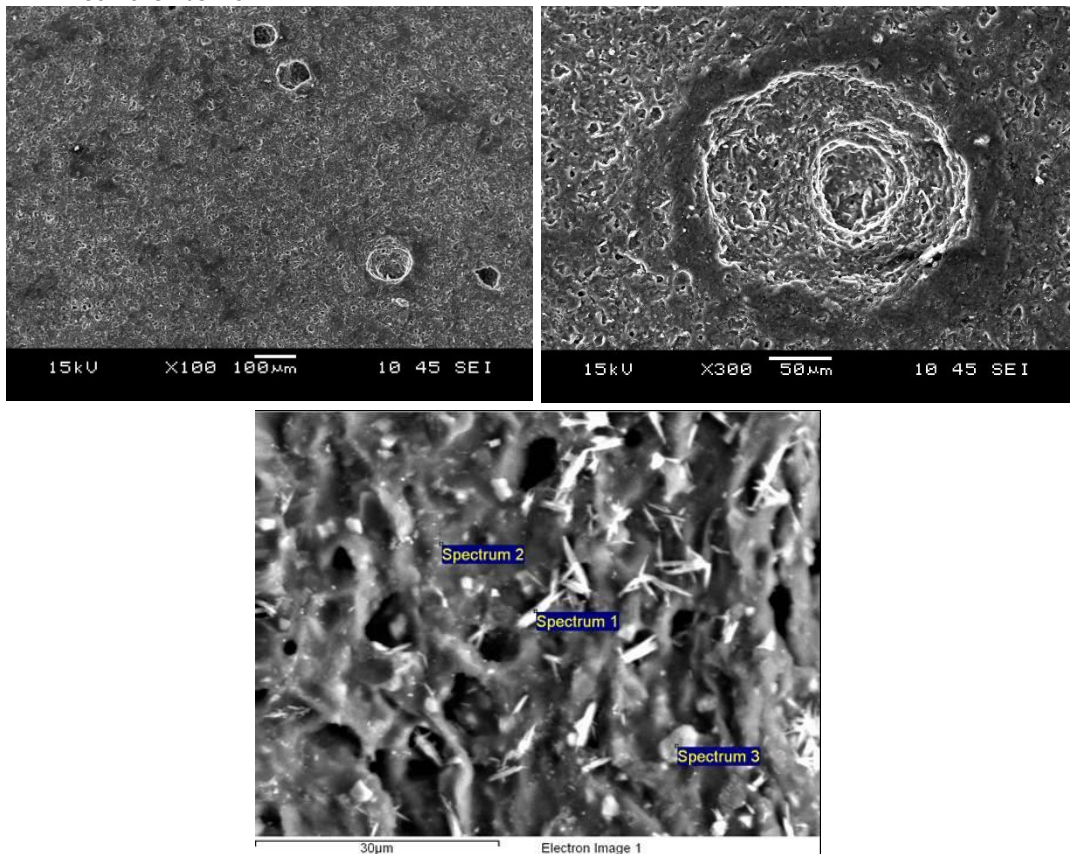


Figure 2.1.60 - SEM images for Xylan0.5wt%GO post-tribocorrosion test, and EDS microanalysis

Spectrum	In stats.	C % wt	O % wt	F % wt	Si % wt	Ca % wt	Mo % wt	Total % wt
1	Yes	26.15	38.99		1.52	21.75	11.58	100.00
2	Yes	34.93			1.91		63.16	100.00
3	Yes	12.97	39.76	2.20	41.31		3.75	100.00

Figure 2.1.61 - Point EDS microanalyses (surface) for Xylan0.5wt%GO post-tribocorrosion

Some Ca based needle-like crystals consistent with the solution composition were identified, that could precipitate since the solution evaporates, and particles containing Mo in the film.

Results for Xylan0.5wtGO, NS4 @80°C: no polarization

Xylan0.5wt%GO coatings have been tested by tribo-tests at 10N load in NS4 solution @80°C following the same procedure previously described but without any polarization. SEM investigation carried out on the cross-section of the specimen.

SEM images are reported in following Figure 2.1.62:

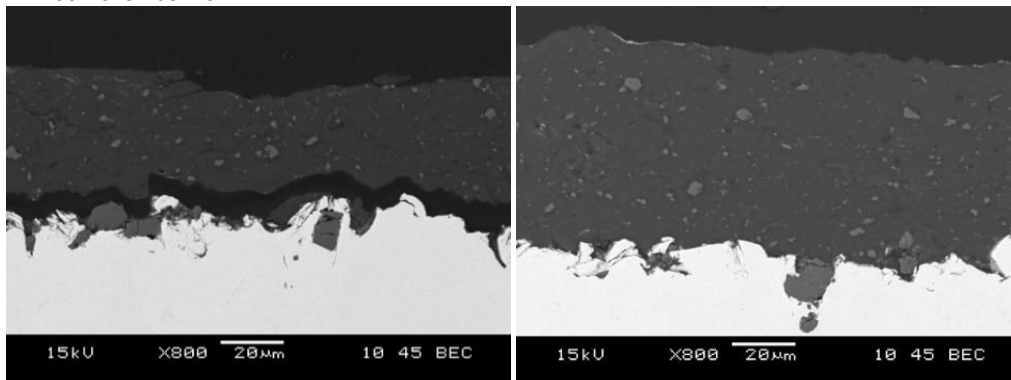


Figure 2.1.62 - SEM cross-section micrographs for Xylan0.5wt%GO coated specimen tested in NS4 @80°C at 10N load. Left: wear track zones. Right: far from the wear track. (Mag. 800X)

The micrographs very clearly show that the coating is detached in area of the wear track and well adhered far from the worn zones. Conversely of what was observed on the tested specimen with polarization, the coating material seems to be not completely worn but presents a 'initial' small wear groove, possibly formed before the detachment of the coating from the substrate.

Importantly, it would seem that the material porosity is less enhanced than in the previous specimen (Figure 2.1.57), that has been worn and polarized.

An explanation of this effect could be differences in the coating initial quality (porosity) not reported, or the added perturbation (although small ± 30 mV vs OCP) introduced in the rubbing system by the polarization of the material, or combined effects in the heated solution, although the polarization applied should be in a potential range commonly considered 'safe' for most of the materials.

Results for Xylan, NS4 @80°C: no polarization

Xylan coatings have been tested by tribo tests at 10N load in NS4 solution @80°C following the same described procedure but without any polarization.

SEM analysis (cross section) evidenced that the coating presents longitudinal cracks in the track zone and it is detached from the substrate. The depth of the wear track is quite small as shown in the images. Far from the worn zones the adhesion of the coating to the substrate looks good.

The coating looks dense as well, with no evident porosities. The EDS microanalysis is reported in Figure 2.1.63.

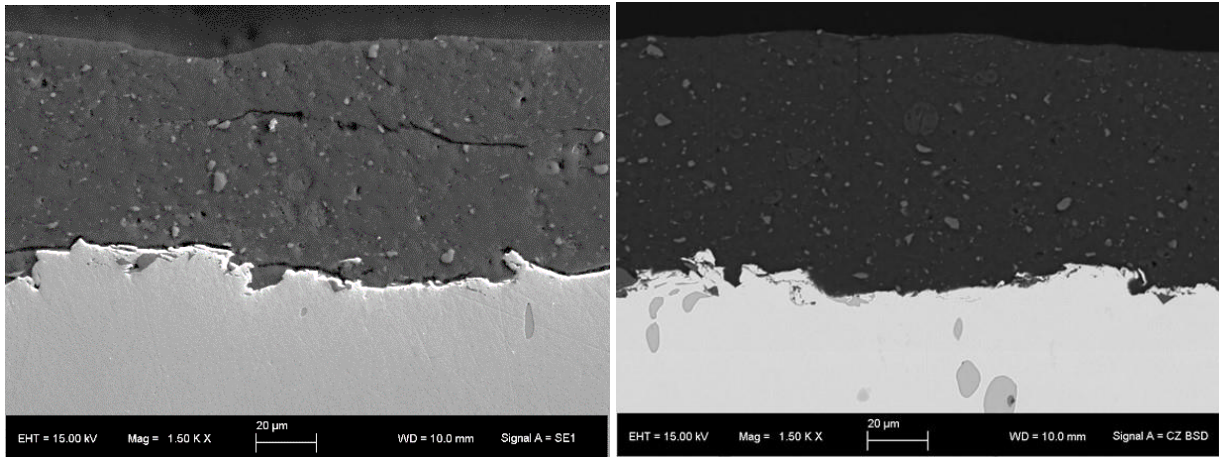


Figure 2.1.63 - SEM micrographs of Xylan coated specimen tested in NS4 @80°C at 10N load. Wear scar zone (left) and far from the wear track (right). Mag. 1500X

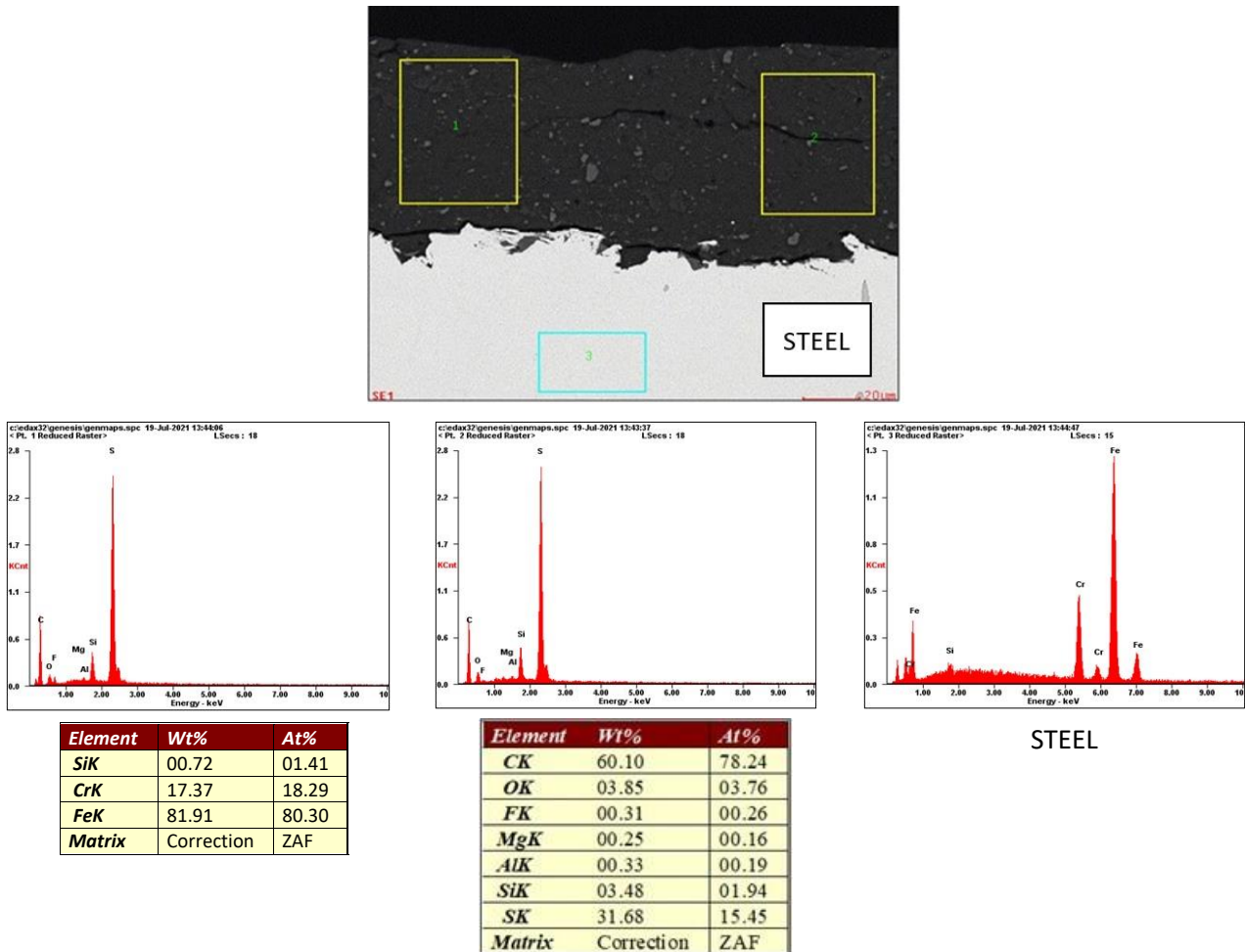


Figure 2.1.64 - EDS area microanalysis for Xylan tested in NS4 @80°C at 10N load.

For xylan coatings the detachment from the substrate was a phenomenon often observed by SEM post-analysis, in tribo-corrosion test carried out in NS4 solution at 80°C. For that reason, corrosion parameters have not been evaluated.

Profilometry

Profilometry investigation was very difficult to carry out for xylan coatings and, for the most, useless for HVOF CerMet specimens due to the reduced depth of wear groove after each step of rubbing. For xylan sometimes the wear tracks were of the same order of magnitude of the specimen initial roughness.

SEM analyses (cross section) was the only effective method for the evaluation of the wear track depth.

Examples of profilometry analyses are reported below, for Xylan0.5wt%GO and Xylan. For Xylan0.5wt%GO and along one diameter (several diameters were checked) the graph evidenced the two tracks, while for Xylan there was no evidence of the wear grooves as shown (Figure 2.1.65 and Figure 2.1.66) :

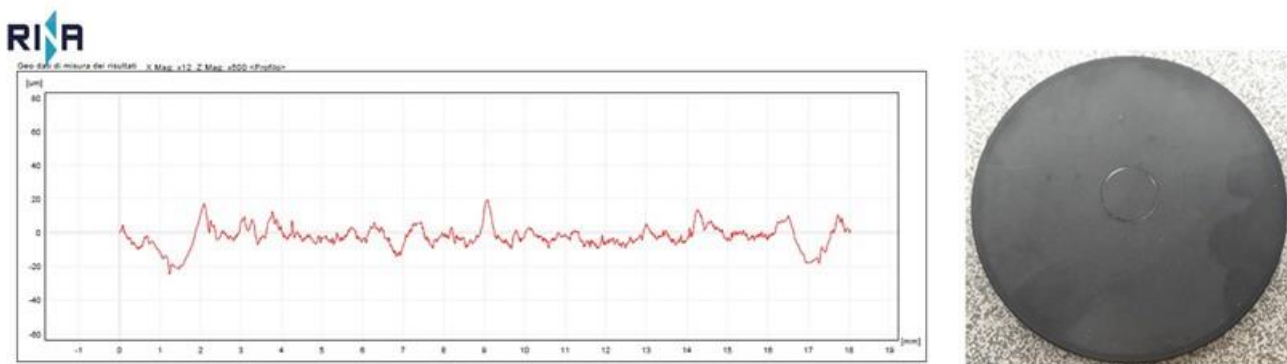


Figure 2.1.65 - Profilometry graph for Xylan0.5wt%GO tested in NS4 @80°C at 10N load. On the right the tested specimen

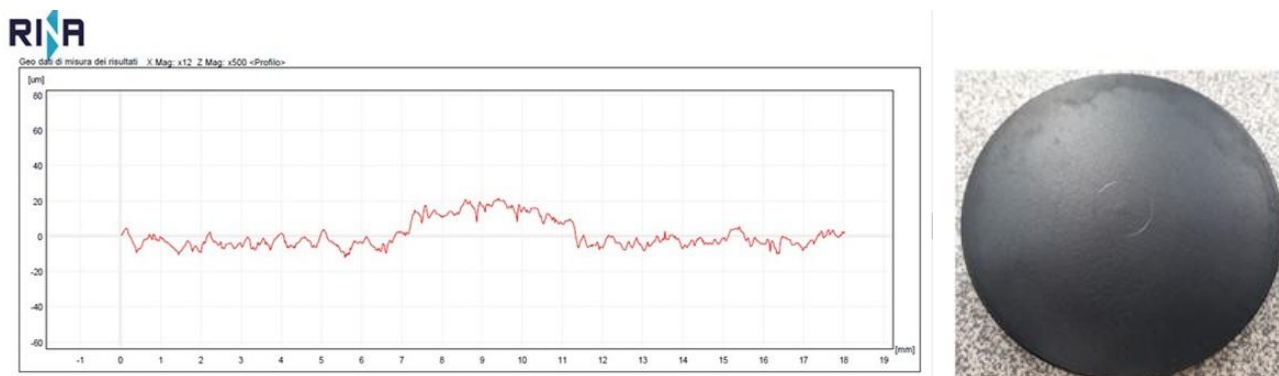


Figure 2.1.66 - Profilometry graph for Xylan tested in NS4 @80°C at 10N load. On the right the tested specimen

The coating deformation due to detachment from the substrate (as revealed by SEM investigation) could be the reason for the incorrect evaluation of the wear track by profilometry.

Results for HVOF CerMet coatings and substrate: weight variation and CoF

To determine the weight variation Δp , each specimen weight was checked before the testing and after each testing cycle. After the first 60 min tests (two cycles) the weight variation is in the following Figure 2.1.67. The substrate shows the tendency to material loss while for both the CerMet coatings a weight gain was evidenced.

After 120 min test (four cycles) the result in terms of weight variation is shown in Figure 2.1.67.

The result is confirmed after 60 min more sliding; at 120 min of testing the substrate has lost 130 mg, while the 232WC (CA3) Cermet specimen has gained 110 mg (Figure 2.1.67):

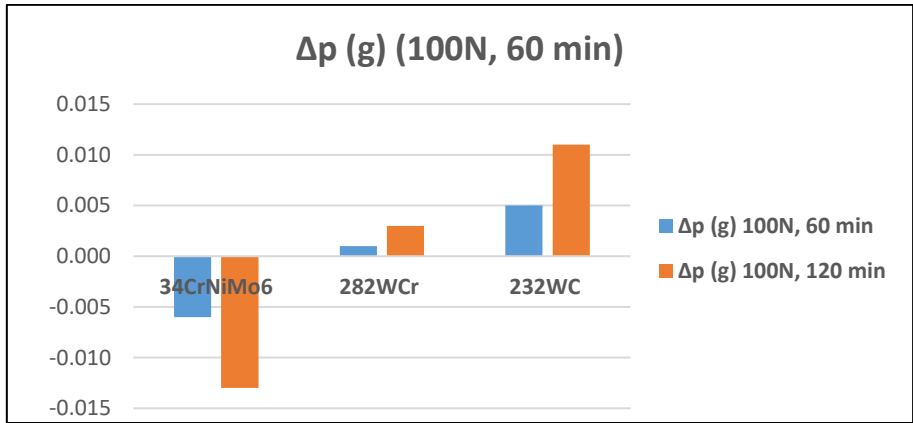


Figure 2.1.67 - The weight variation after two cycles (four step) tribo corrosion tests of 30 min duration each

The Friction coefficient CoF average values recorded are summarized in the following Figure 2.1.68 :

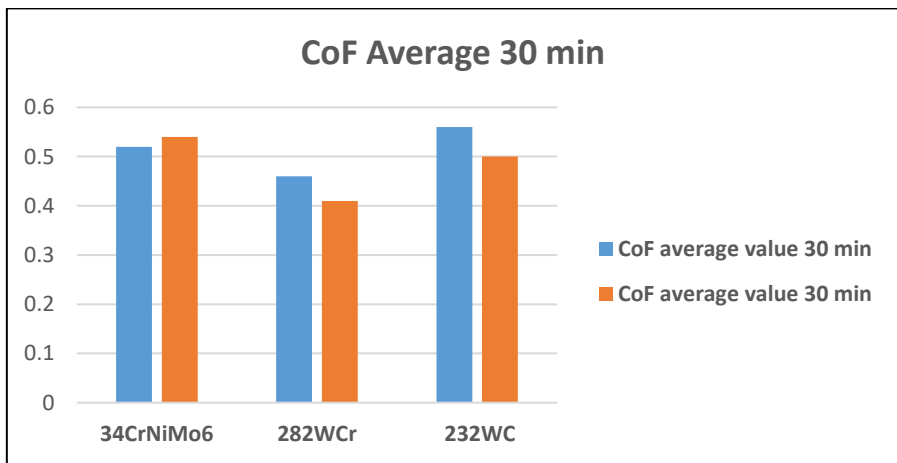


Figure 2.1.68 - Average values of Friction Coefficient recorded for the tested HVOF coating materials and steel substrate

As an example, herein a CoF plot for a single step of the steel substrate (Figure 2.1.69):

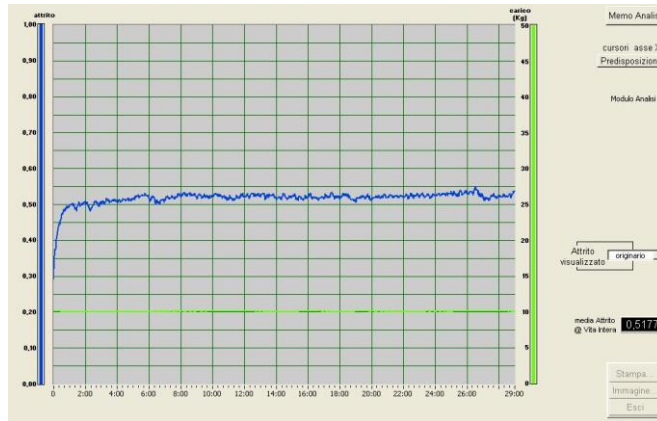


Figure 2.1.69 - The CoF plot with the curve for 34CrNiMo6 steel substrate single wear step 30 min lasting. The load is in Kg

Results for HVOF CerMet coatings and substrate, NS4 @80°C: tribocorrosion

For the substrate 34CrNiMo6 the curves OCP (open circuit potential) and PD (potentiodynamic) of the multistep experiment summarized in Table 2.1.22 are reported in Figure 2.1.70 .

The total duration of the wear test for these specimens was 120 min, load 100 N @ 80°C. A first investigation by SEM was carried out after the first 60 min rubbing. Since the damage was almost undetectable, the test was repeated on the same specimen and for 60 more minutes, in the same experimental conditions.

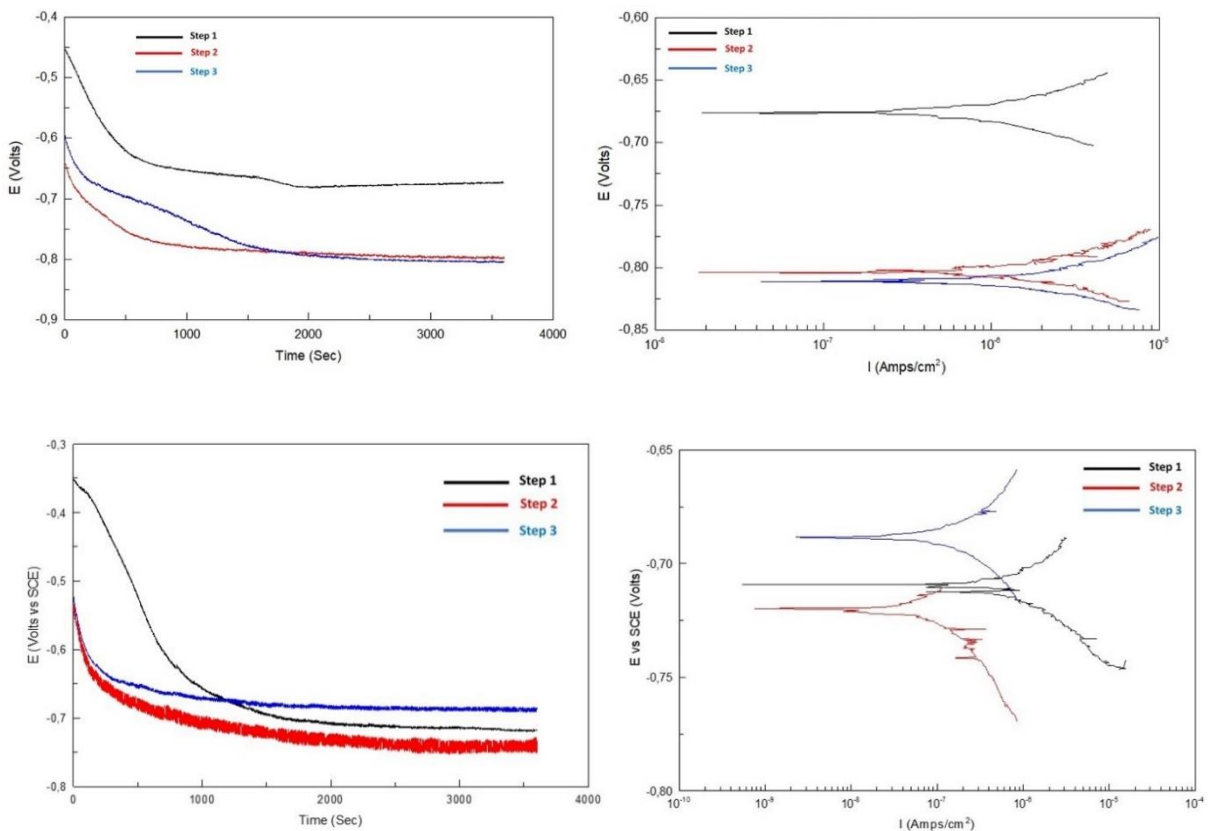


Figure 2.1.70 - OCP and PD curves for 34CrNiMo6 steel substrate: upper the first three step test. Lower: the second series of step test

For the CerMet 232WC the wear after the first 60 min rubbing was quite undetectable; the same happened for 282WCr. For both the coatings a second group of tests was then carried out.

As an example, curves of OCP and PD relatively to one series of tests are shown for the two class of CerMets in Figure 2.1.71 :

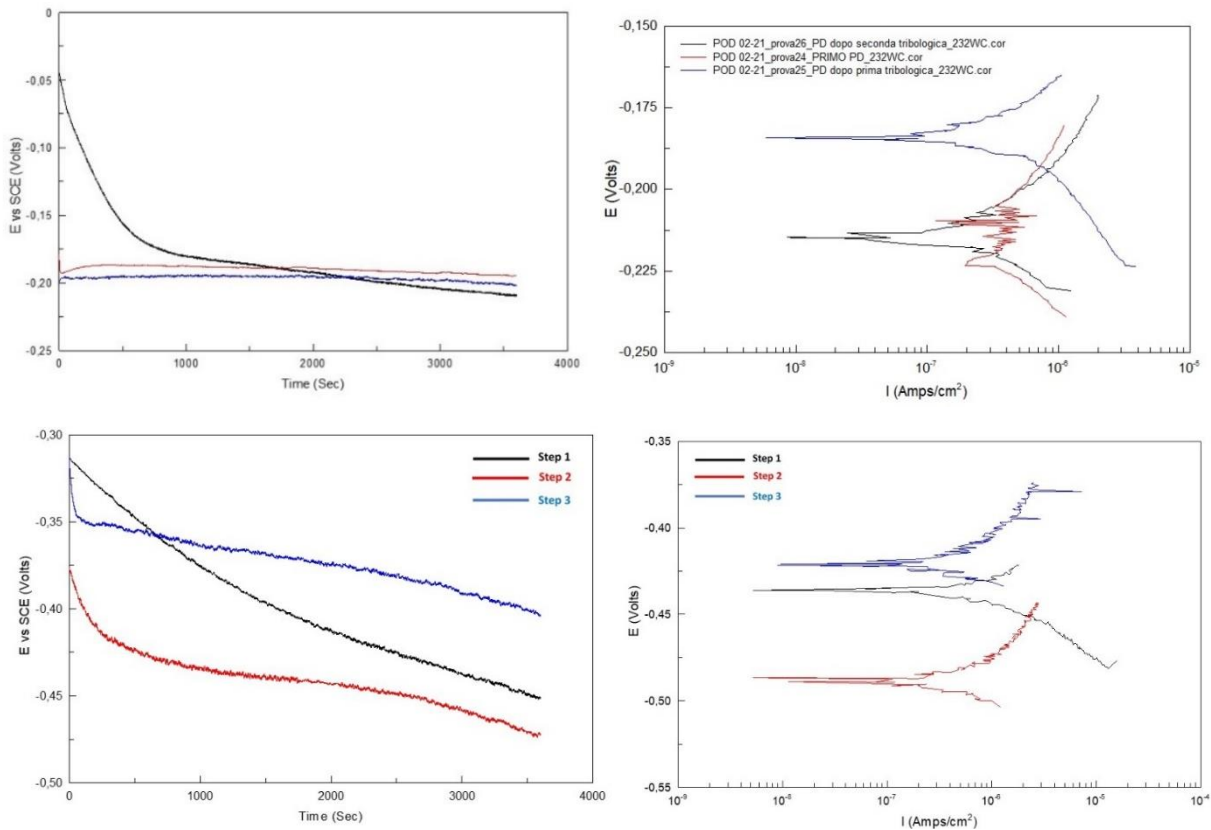


Figure 2.1.71 - One set of OCP and corresponding PD curves: upper 232WC. Lower: 282WCr

The curves reported in Figure 2.1.70 and Figure 2.1.71, are quite representative of the trend observed for each material, tested in the selected conditions (normal load, temperature, polarization, solution..), although the investigation to determine the morphology of the wear track in the tested specimens revealed some aspects, as will be explained, that have to be considered as integration of the results from the PD curves (fitting) analysis.

In the following Table 2.1.23 the OCP values are averaged for the steel substrate and for the CerMet coatings:

Table 2.1.23 - Average OCP values for the tested materials

Material	OCP, V
34CrNiMo6	-0.717
282WCr	-0.442
232WC	-0.232

The OCP for the three materials stabilize at a more negative value with respect of the starting OCP (before wear) values: this is particularly evident for the steel (300 mV drop).

The evaluated current densities are very similar for the three classes of materials and showed a slightly higher average IO value for 282WCr. However, it was observed that the OCPs for this coating could not reach a stable value in the time interval between two wear steps.

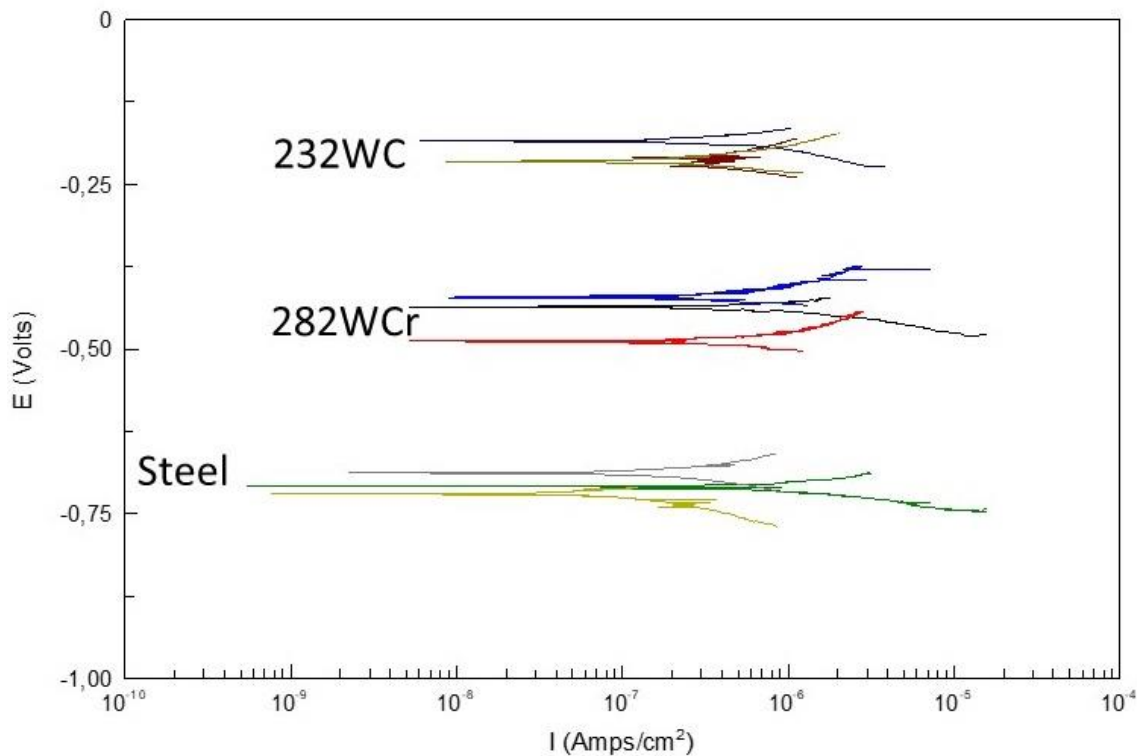


Figure 2.1.72 - The PD curves grouped for the Steel substrate and for the 232WC and 282WCr coatings

As shown in Figure 2.1.67 the measured weight variation is negative (weight loss) for the steel substrate only, while the CerMets show the tendency to weight gain, especially 232WC.

As revealed by SEM the analysis of the wear track (Figure 2.1.73) evidenced for the steel a well-defined track (the grinding lines are flattened by the counterpart during the test), while the CerMets coatings are strongly resistant to the effect of applied load and sliding. However, the surfaces of both 232WC and 282 WCr are plenty of cracks (Figure 2.1.74), and this net-like cracked structure is detrimental for the protection of the substrate against corrosion.

In fact, especially in the wear track area, mixed oxides containing Fe and Cr were detected, especially they seem to be in a higher amount in 282 WCr than in 232WC.

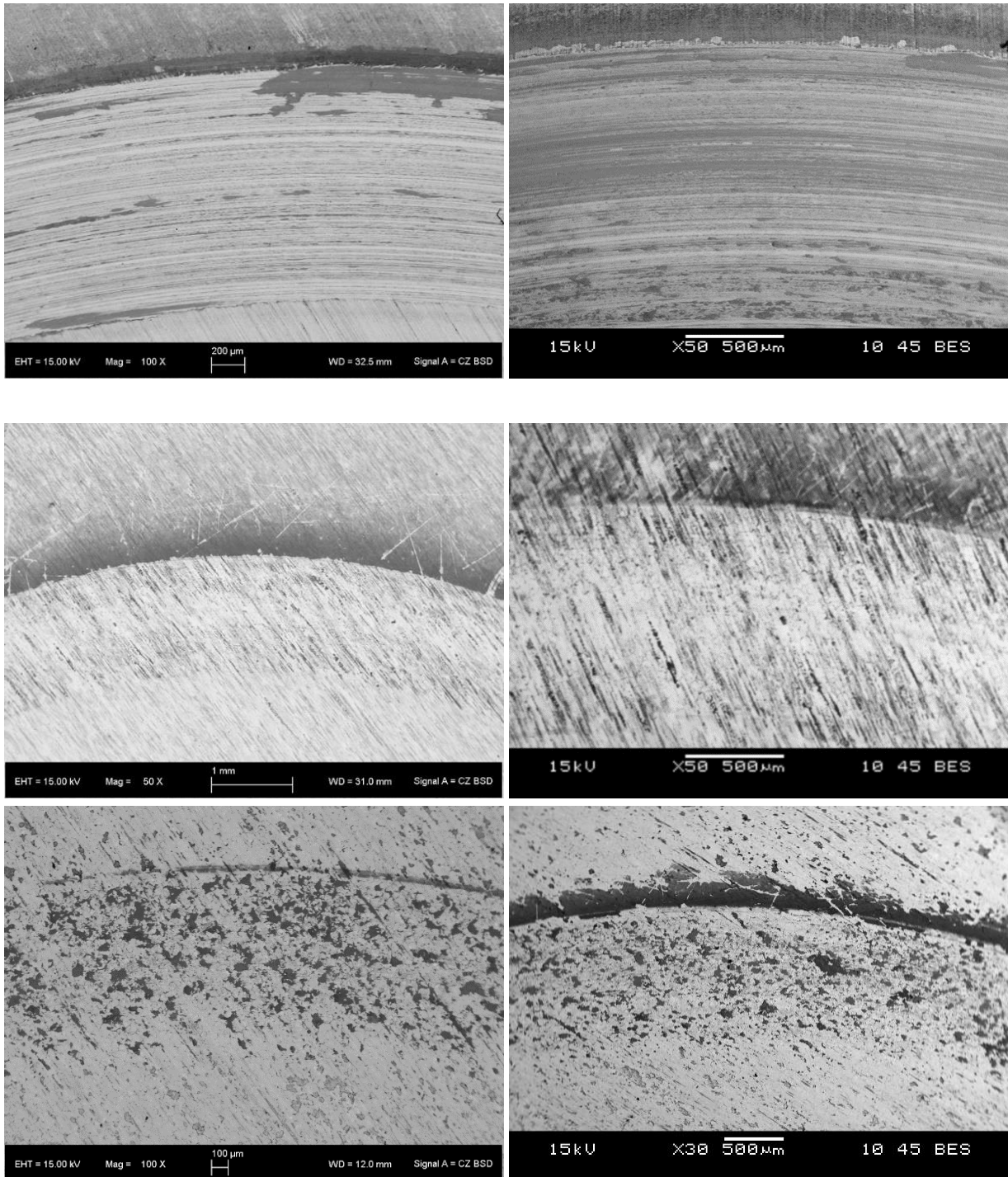


Figure 2.1.73 - SEM Micrographs of track zone for tested 34CrNiMo6 steel, 232WC (middle) and 282WC coatings (lower).

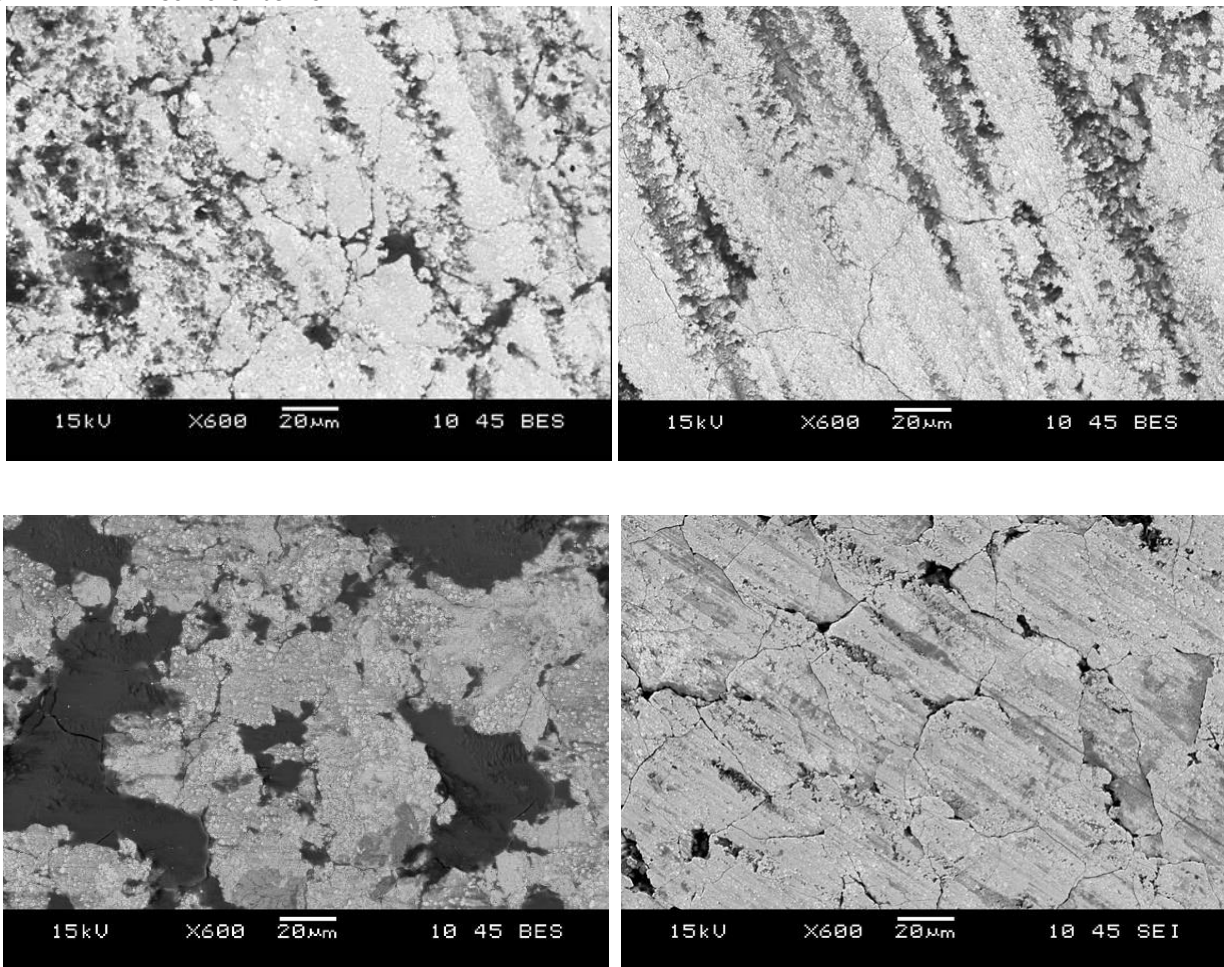
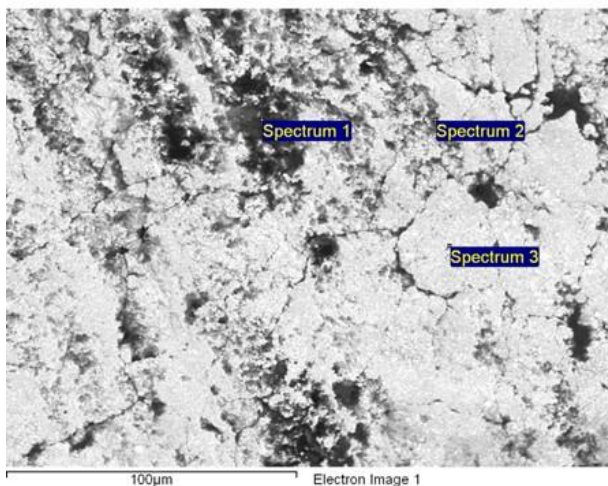


Figure 2.1.74 - SEM Micrographs of tested 232WC (upper) and 282WCr coatings (lower). Area inside the wear track (left) and outside the wear track (right)

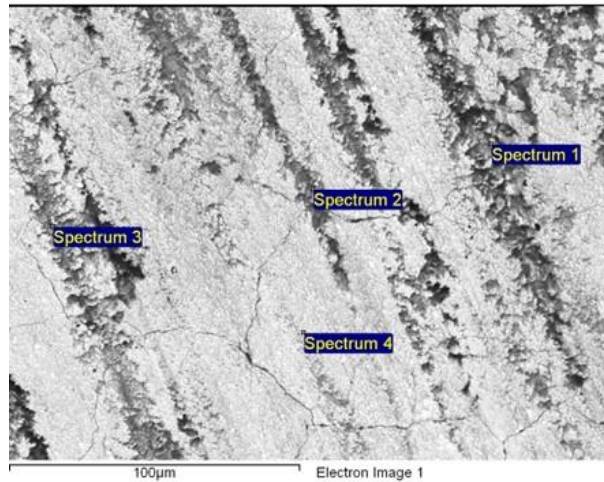
EDS analysis better identify the dark phases well recognizable in the micrographs collected in backscattered mode.

For 232WC EDS analysis reported below evidenced some iron (mixed oxides) in the wear track and outside the wear track, while other deposited material are residuals from the solution (Figure 2.1.75 and Figure 2.1.76).



Spectrum	In stats.	O	Mg	Al	Ca	Cr	Fe	Co	W	Total
1	Yes	34.37	6.16	5.02	0.62	7.29		12.97	33.57	100.00
2	Yes	23.87	4.56	1.34		4.47	4.97	13.36	47.43	100.00
3	Yes	1.88				2.31		6.39	89.41	100.00

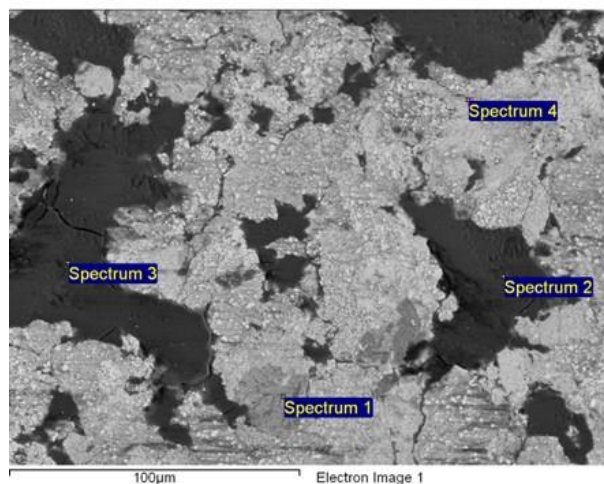
Figure 2.1.75 - EDS microanalysis for worn 232WC in the wear track area



Spectrum	In stats.	O	Mg	Al	Cr	Fe	Co	W	Total
1	Yes	14.56	3.77	1.12	5.20		20.53	54.82	100.00
2	Yes	18.31	2.77		2.63	1.71	9.75	64.83	100.00
3	Yes	14.34	2.71	0.93	5.02		13.22	63.79	100.00
4	Yes	2.67			1.56		4.03	91.74	100.00

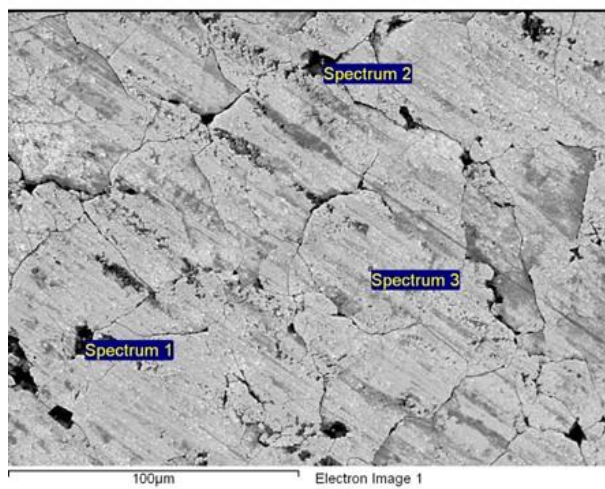
Figure 2.1.76 - EDS microanalysis for worn 232WC outside the wear track area

For 282WCr sample, EDS analysis reported below evidenced higher amount of iron (mixed oxides) in the wear track, if compared to 232WC, while outside the wear track no iron was found. Some zones with chromium oxide were identified (Figure 2.1.77 and Figure 2.1.78).



Spectrum	In stats.	O	Mg	Al	Cl	Ca	Cr	Fe	Ni	W	Total
1	Yes	2.07					51.55			46.38	100.00
2	Yes	32.87	6.13	2.09		0.85	29.12	10.74	8.02	10.18	100.00
3	Yes	35.72	6.96	2.12	0.57	0.99	26.83	9.75	8.89	8.15	100.00
4	Yes	6.03	0.65				20.77		11.07	61.49	100.00

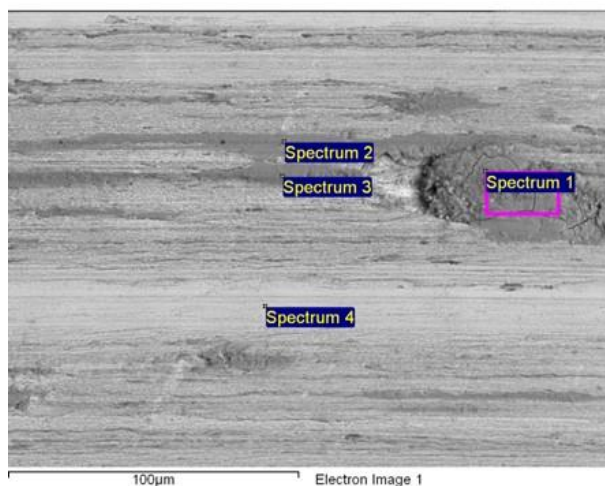
Figure 2.1.77 - EDS microanalysis for worn 282WCr in the wear track area



Spectrum	In stats.	O	Mg	Al	S	Cl	Ca	Cr	Ni	W	Total
1	Yes	18.73	6.54	2.38	0.78	3.25		22.14	6.21	39.98	100.00
2	Yes	29.85	10.61	5.10		2.62	7.42	16.14	5.08	23.19	100.00
3	Yes	3.08						22.57	9.41	64.95	100.00

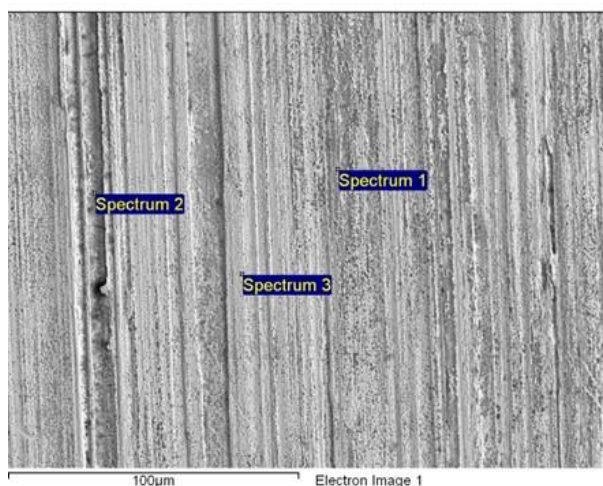
Figure 2.1.78 - EDS microanalysis for worn 282WCr outside the wear track area

Finally, for the substrate 34CrNiMo6 steel (Figure 2.1.79 and Figure 2.1.80) the growth of mixed oxides, mainly Fe based (expected) were present in the wear track, while a reduced oxidation was detected outside the wear track.



Spectrum	In stats.	O	Mg	S	Cr	Fe	Ni	Total
1	Yes	21.31	0.90	0.43	1.52	75.84		100.00
2	Yes	20.56	0.82	0.55	2.09	75.98		100.00
3	Yes	20.63	0.91		1.63	76.83		100.00
4	Yes	2.88			1.28	93.80	2.05	100.00

Figure 2.1.79 - EDS microanalysis for worn 34CrNiMo6 steel in the wear track area



Spectrum	In stats.	O	Mg	Cr	Mn	Fe	Total
1	Yes	5.80	2.09	2.54	0.94	88.62	100.00
2	Yes	5.52	2.69	1.46	0.84	89.49	100.00
3	Yes	2.23	0.60	1.67		95.49	100.00

Figure 2.1.80 - EDS microanalysis for worn 34CrNiMo6 steel outside the wear track area

Present paragraph refers to the activity and the results concerning investigation carried out on Xylan+0.5wt%GO and down-selected CerMet based coatings deposited on 34CrNiMo6 steel substrate to assess the effect of tribocorrosive phenomena at elevated temperature. For the investigated materials a modified protocol was tuned, since the combination material/experimental conditions (solution, temperature, sliding) were not suitable for quali-quantitative evaluation of the degradation occurred according to a traditionally accepted protocol. The modified protocol cannot be intended as an alternative way to assess tribocorrosion because materials were investigated in the time interval after the phenomena have occurred and a certain recovery could have taken place.

Based on the investigations on slide/corrosive phenomena, the following main conclusions are drawn:

- The investigation aimed at the evaluation for the tested materials of the damage due to tribocorrosive phenomena in NS4 solution at 80°C and in the selected experimental conditions of load and relative speed of the counterpart, in ball-on-disk tests.
- The investigation has been carried out by step of wear alternate to corrosion measurements or by evaluation of the damage after simple wear tests in the selected solution at 80°C (no polarization).

- For Xylan based compounds (0wt% and 0.5wt%) the effect of small polarization seems to have some influence with a modification of the material (more porosity) although the experiments have been conducted in a narrow potential interval close (± 30 mV vs OCP) generally considered safe. The modified Xylan (Xylan0.5wt%GO) looks worn out in the track area, while all analyzed coatings look detached from the substrate in the track area, where the material was stressed by the application of the load (10N). Far from the wear track zone the coating adhesion is good.
- For CerMet coatings (232WC, 282WCr) the analysis after tests showed some weight gain. SEM investigation on the coating surface evidenced a 'net of cracks' both in the wear track and out of the wear zone for both 232WC and 282WCr. The coatings in such conditions are not fully protective toward the substrate since Fe in mixed oxides has been detected by EDS analysis.
- 232WC in the wear track area looks less affected by oxidation if compared to 282WCr in the same area, while 282WCr seems less affected outside the wear track. At the same time in 282WCr cracks in the track appears to be more affected by the sliding (more damaged).
- 232WC showed higher weight gain with respect to 282WCr, but higher OCP equilibrium value.
- Conversely, steel substrate weight loss was consistent with the phenomena of wear and maybe material loss in the wear track. The 34CrNiMo6 steel shows the more negative OCP potential value after stabilization vs both coatings and the higher weight loss.

2.2 T3.2 Corrosion testing in simulated geothermal drilling environment

Led by UoI, in this task the corrosion testing equipment was set up and test conditions designed to test the GeoDrill coatings produced in WP2 in simulated geothermal drilling environment. The corrosion tests of the developed GeoDrill coatings were carried out in simulated geothermal drilling environment at elevated temperature and pressure. The characteristics of the prepared simulated geothermal drilling environment in the laboratory for the corrosion coupon testing was based on real field conditions. A description of the test conditions and list of samples tested is shown in Table 2.2.1, the low alloyed carbon steel substrate is labelled as A7.

Table 2.2.1 Testing information in T3.2

Sample ID	Autoclave test	Autoclave test
A7	Liquid phase at P=50 barG (N ₂), T=120 °C; for 14 days (without corrosive gases)	Vapor- Liquid at P=50 barG (N ₂), T=250 °C; for 7 days (with corrosive gases: H₂S, CO₂)
0wt%GO		
0.5wt%GO		
1wt%GO		
2.5wt%GO		
5wt%GO		Vapor- Liquid at P=50 barG (N ₂), T=250 °C; for 7 days (without corrosive gases) And Vapor- Liquid at P=50 barG (N ₂), T=250 °C; for 7 days (with corrosive gases: H₂S, CO₂)
232WC_A7		
233CrC_A7		
282WCr_A7		
234Flux_A7		
235Amor_A7		
283HEA_A7		
HP-LPPTFE_A7		
HP-HPPTFE_A7		

The design and setup of the high temperature and pressure corrosion testing facility at University of Iceland is shown in Figure 81.



Figure 81 Design and setup of the high temperature and pressure corrosion testing facility at University of Iceland.

The preliminary results from the visual inspection and weight loss/gain analysis were the following:

- Samples with 0.5% GO Xylan-GO coated samples showed promising performance with least visible changes in coating appearance and weight change.
- The 282WCr; 233CrC and 283HEA samples were the best performing HVOF fabricated samples, with least visible changes in coating appearance compared to untested samples and for the 282WCr no crevice corrosion damages were visible.
- The ENP coatings had visible corrosion damages for all designed test conditions.

The tested corrosion coupons were used for evaluating the corrosion resistance with microstructural and chemical compositional analysis performed in Task 3.5. The results were used for the ranking of the coatings to select the best coatings for the components of the prototypes of the novel DTH hammer developed and built in WP4.

2.3 T3.3 Erosion-corrosion testing in simulated geothermal drilling environment

Led by TWI, work in this task was carried out on erosion-corrosion testing of WP2 developed coatings in simulated geothermal drilling environment. Detailed results have been reported in D3.3 - Report on erosion-corrosion testing of samples in simulated environment, including the following:

- Design of an erosion-corrosion testing facility using main elements of the slurry pot equipment (ASTM G119), with in-situ electrochemical measurement capabilities.
- Define formulation of simulated geothermal drilling fluid to be used in erosion-corrosion testing.
- Preliminary erosion-corrosion testing at 24h duration in simulated drilling fluid on a total number of sixteen (16) samples, including three types of steels for benchmarking and thirteen (13) samples deposited with coatings developed in WP2. Among those, six (6) samples including Steel 1, 222Xylan/GO1, 232WC1, 234Flux1, Steel 2, and 232WC2 were down-selected for further testing.
- Further erosion-corrosion testing was carried out for 7 days to evaluate how down-selected samples perform in simulated drilling environment for longer-term. From the results, samples 222Xylan/GO1 and 234Flux1 are proved to have good protection to Steel 1 in the selected testing condition. Steel 2 performs very well itself and is recommended not to have the need to be coated in similar drilling environment.
- Ranking and recommendations from this deliverable report is based on results from erosion-corrosion testing in simulated geothermal drilling environment only. Final decisions on material ranking should be based on overall performance of all environmental testing in WP3, which will be put together in D3.5.

2.4 T3.4 HTHP testing and evaluation of sensor and cable material

Led by GER, in this task samples of cable and sensor materials, down selected for innovative sensors developed by PVI for the GeoDrill project, were tested in laboratory by Gerosion in collaboration with University of Iceland in high temperature and pressure conditions (Figure 82, Figure 83), commonly encountered during drilling operations. The samples were also exposed to conditions defined as non-standard, at a temperature of 250°C and with CO₂ (carbon dioxide) and H₂S (hydrogen sulphide) introduced to the system simulating geothermal gas and a two-phase environment. The results were presented, discussed and recommendations given based on the material performance and its failure analysis.



Figure 82 Oven used for lower T settings. Humidity level can be controlled.



Figure 83 Autoclave setup used for simulating drilling environment.

2.5 T3.5 Evaluation and ranking of developed materials and coatings

Led by UoI, the following tasks were performed in T3.5; a) the evaluation of the corrosion resistance of the coatings tested in HTHP simulated geothermal drilling environment by UoI summarized in Task 3.2; and b) ranking of the developed materials and coatings by best performance based on microstructural characterization, mechanical properties and corrosion and wear resistance measured in laboratory tests in Tasks 3.1, 3.3 and 3.4. The recommendation from the work within this task will be used as an input for WP4 in the making of the prototypes of the novel DTH hammer.

For task a) the following conclusions were made based on comparison of micro-structure of non-tested samples from Task 3.1 and on comparison between the coatings and substrate material:

- In the simulated conditions for normal drilling operation; at 120°C in water:
 - All the HVOFs; 232WC, 233CrC, 282WCr, 234Flux, 235Amor and 283HEA performed well with no corrosion damage and only a minor increased amount of oxygen detected in the chemical composition analysis with EDS of the corrosion tested samples.
 - The heat treated ENP coatings (HP-LP-300, HP-HP-300) did not perform adequately since the coatings had high amount of Ni-oxides formed on the surfaces and the HP-

Date: 30 November 2021

HP-300 experienced delamination and breakage and allowed diffusion of corrosive species to react to the substrate. The HP-LP-300 performed better compared to HP-HP-300, with less corrosion damage; only small cracks present on the surface and no corrosion of the substrate.

- Compared to the non-GO containing Xylan coating and the higher GO wt% Xylan coatings the 0.5wt% and 1wt% Xylan-GO showed the least effect of corrosion indicated by the lowest weight loss and no cracks or delamination or breakage in the film detected. All the Xylan coatings did though have some dissolution and ingress of corrosive species in the coating (permeable) since Fe, Ni, O were detected on the surface of all coatings to some extent. Overall the 1wt% Xylan coating allowed least corrosion of the substrate material.
- In the simulated conditions for drilling operation at high temperatures, 250°C , in geothermal fluid/vapour with H_2S and CO_2 :
 - For the HVOFs; the 233CrC, 282WCr, and 283HEA performed the best. They all contained though small amount of sulfur (S) and increased amount of oxygen (O) compared to the untested samples indicating some reactions to the H_2S and CO_2 . The surface of the tested 232WC sample was covered with a thin cobalt sulfur rich layer with few large crystals rich in W-O. Also for the 234Flux coating a thick nickel (Ni) sulfide (S) rich corrosion film formed on the surface, indicating active corrosion of the coating to certain extent. A more porous structure was observed for the 235Amor coating compared to the un-tested sample with ingress of corrosive species detected in the cross-section analysis close to the surface.
 - The Xylan-GO 0.5wt% and 1wt% were less effected by the corrosive environment compared to the 2.5wt% GO and the neat Xylan (0wt% GO). All the coatings though experienced weight loss and the surfaces contained Fe, S rich corrosion products. Also, corrosion products were detected in the cross-section of the coatings and interfacial damage (corrosion of substrate) indicate the permeability of the coatings. Additionally, although the thickness of the coatings reduced, the continuous layer and less interfacial damage was observed for the 0.5wt%GO compared to the 1wt% GO coating.
- Results from additional tests performed for the ENPs and HVOFs at 250°C and 50 bar with N_2 , but without the corrosive gases showed:
 - All the HVOFs; 232WC, 233CrC, 282WCr, 234Flux, 235Amor and 283HEA performed well with no corrosion damage and only a minor increased amount of oxygen detected in the chemical composition analysis with EDS of the corrosion tested samples.
 - The heat treated ENP coatings (HP-LP-300, HP-HP-300) did not perform adequately since the coatings had high amount of precipitates and Ni-oxides formed on the surfaces. The HP-HP-300 had extensive Ni-O rich crystals growing on the surface of the coatings indicating degradation of the coating in the HTHP environment.

The results from deliverable D3.1 and D3.3 were used along with the corrosion analysis results for ranking the coatings to select the most potential coating candidate of each coating group for further test in in-situ in drilling tests by applying them to the prototype of the novel DTH hammer components in WP4.

The following conclusions were made based on the ranking based on the various tests performed within WP3:

- The Xylan 0.5wt%GO is the most potential coating showing best performance among the Xylan based polymer coatings developed within Geo-Drill. Thus it should be tested further in-situ in DTH hammer prototype in WP4 where low friction is needed and erosion-corrosion can be encountered.
- The most promising HVOF coating developed within the Geo-Drill and recommended to be tested further in-situ where high wear is encountered in high temperature water based drilling fluid for the protection of 34CrNiMo6 substrate is the 234Flux coating.
- The HP-LP-PTFE300 showed better performance than the HP-HP-PTFE300 coating with good corrosion and wear resistance at RT conditions but does poorly at higher temperatures and pressure which restrains the potential usage for geothermal drilling conditions.
- For the sensor material the selected materials performed well under standard drilling conditions based on failure analysis except the silicon material and the Kapton which showed decrease in ductility.

2.6 T3.6 Perform welding test on coupons

Led by TWI, work in this task was carried out on welding processing and results are detailed in D3.6 – Impact of welding on coating integrity, including the following:

- Welding processes were reviewed in the context of the materials and geometry of the drill pipe components.
- Following the review, Rotary Friction welding was selected as the most suitable process.
- Rotary friction welding was used to produce test coupons, parameters were selected to form a Design of Experiments (DoE) matrix.
- All the welding parameters selected achieved a uniform, defect-free weld.
- DoE software was employed to optimise parameter selection in relation to peak hardness and ultimate tensile strength.
- Weld coupons were made using optimised parameters for testing of a WC-CoCr coating (36WC) and a self-fluxing coating (36Flux) coating.
- The rotary friction welding process does not seem to have an impact on the coating integrity. Both cermet and alloy HVOF sprayed coatings seem to behave similarly close to the weld interface (at the Heat Affected Zone or HAZ) as compared with the parent metals.
- This task has increased the consortium's understanding of the effect of welding on coating integrity.

3 CONCLUSIONS

In this work package, a range of materials and coatings that were developed in WP2 were characterised and tested under different conditions. Conclusions drawn from this WP are:

T3.1: Based on the results from the microstructural, mechanical, and dry PoD sliding test the 1-3 best performing coatings per coating group were selected for further testing at high temperatures and tribo-corrosion sliding tests. The Xylan+0.5wt% GO coating was chosen from the Xylan-GO coating group and the heat treated ENPs (at 300°C); HP-HP-PTFE 300 and HP-LP-PTFE 300. The HVOF coatings selected for further tests were the 233WC, 234Flux and 282WCr coatings.

T3.2: Preliminary results from visual inspection and weight loss/gain analyse after corrosion testing show that:
1) Samples with 0.5% GO Xylan-GO coated samples showed promising performance with least visible changes

in coating appearance and weight change, 2) The 282WCr; 233CrC and 283HEA samples were the best performing HVOF fabricated samples, with least visible changes in coating appearance compared to untested samples and for the 282WCr no crevice corrosion damages were visible, 3) The ENP coatings had visible corrosion damages for all designed test conditions, 4) The tested corrosion coupons were used for evaluating the corrosion resistance with microstructural and chemical compositional analysis performed in Task 3.5.

T3.3: An erosion-corrosion testing facility using main elements of the slurry pot equipment (ASTM G119) was designed, with in-situ electrochemical measurement capabilities. Formulation of simulated geothermal drilling fluid was defined for erosion-corrosion testing. A total number of sixteen (16) samples were tested at 24h duration in simulated drilling fluid, with six (6) were down-selected for 7day testing. From the results, samples 222Xylan/GO1 and 234Flux1 are proved to have good protection to Steel 1 in the selected testing condition. Steel 2 performs very well itself and is recommended not to have the need to be coated in similar drilling environment.

T3.4: From HTHP testing, the materials were exposed to a simulated geothermal well drilling environment commonly encountered during drilling operations of geothermal wells, as well as conditions that occur in an extreme scenario such as during ingress of geothermal gases and high temperatures (250°C). The results give information on the stability and chemical resistance of the sensor materials towards the environment developed in geothermal well drilling.

T3.5: The following conclusions were made based on a) evaluation of the corrosion resistance of the coatings received from WP2 after corrosion testing in simulated geothermal drilling environment at elevated temperature and pressure in Task 3.2; and b) the ranking of the developed materials and coatings by best performance based on microstructural characterization, mechanical properties and corrosion and wear resistance measured in laboratory tests in Tasks 3.1, 3.3 and 3.4:

- The Xylan 0.5wt%GO is the most potential coating showing best performance among the Xylan based polymer coatings developed within Geo-Drill. Thus it should be tested further in-situ in DTH hammer prototype in WP4 where low friction is needed and erosion-corrosion can be encountered.
- The HVOF coating developed within the Geo-Drill recommended to be tested further in-situ for the first proto-type of the DTH hammer where high wear is encountered in water based drilling fluid for the protection of 34CrNiMo6 substrate is the 234Flux coating.
- The HP-LP-PTFE300 showed better performance than the HP-HP-PTFE300 coating with good corrosion and wear resistance at RT conditions but does poorly at higher temperatures and pressure which restrains the potential usage for geothermal drilling conditions.
- For the sensor material the selected materials performed well under standard drilling conditions based on failure analysis except the silicon material and the Kapton which showed decrease in ductility.

T3.6: Rotary friction welding has proved capable of creating high integrity, uniform, and defect free joints. Moreover, rotary friction welding process is not seen to have an impact on the coating integrity. Both cermet and alloy HVOF sprayed coatings seem to behave similarly in the heat affected zone as compared with parent metals.

REFERENCES

There are no sources in the current document.

[1] R.N.Parkins, "Environmental sensitive cracking Low-pH SCC of high pressure pipelines", Battelle NG18 Report 191, August 1990